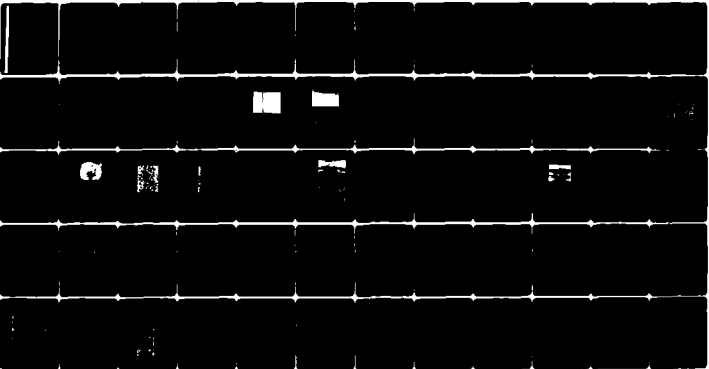


13-0004 780

CHARLES STARK DRAPER LAB INC CAMBRIDGE MA F/S 17/7  
MATERIALS RESEARCH FOR ADVANCED INERTIAL INSTRUMENTATION. TASK ---ETC(U)  
OCT 79 D DAS, K KUMAR, E WETTSTEIN, J WOLLAM N00014-77-C-0388  
R-1330 ML

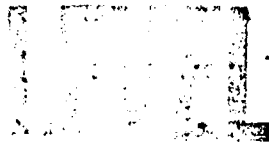
UNCLASSIFIED

[ of ]  
254/780



END  
DATE  
FILMED  
7-80  
DTIC

ADA 084780



# (12)

(14)

R-1330

AD61775  
1 6 11 19  
AD61 6 1 1 0

STask 3-108-968

(6) MATERIALS RESEARCH FOR ADVANCED  
INERTIAL INSTRUMENTATION.

TASK 2. GAS BEARING MATERIAL  
DEVELOPMENT BY SURFACE  
MODIFICATION OF BERYLLIUM.

(9) TECHNICAL REPORT, NO. 2,  
FOR THE PERIOD  
1 OCTOBER 1978, TO 30 SEPTEMBER 1979,  
BY

(10) D. DAS, K. KUMAR, E. WETTSTEIN, J. WOLLAM

(11) Oct '79

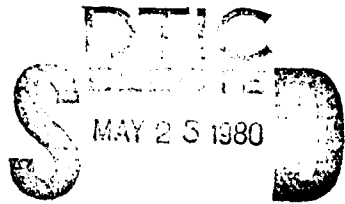
Prepared for the Office of Naval Research,  
Department of the Navy, Under Contract  
N00014-77-C-0388

(15)

(12) 7A

Approved for Public Release; Distribution Unlimited.

Permission is Granted the U.S. Government to  
Reproduce This Paper In Whole Or In Part.



A

The Charles Stark Draper Laboratory, Inc.  
Cambridge, Massachusetts 02139

DDC FILE COPY,

80 5 23 033

408386

mt

REPORT DOCUMENTATION PAGE		READ INSTRUCTIONS BEFORE COMPLETING FORM
1. REPORT NUMBER Technical Report No. 2	2. GOVT ACCESSION NO. AD-A084780	3. RECIPIENT'S CATALOG NUMBER
4. TITLE (and Subtitle) MATERIALS RESEARCH FOR ADVANCED INERTIAL INSTRUMENTS TASK 2. GAS BEARING MATERIAL DEVELOPMENT BY SURFACE MODIFICATION OF BERYLLIUM	5. TYPE OF REPORT & PERIOD COVERED 1 October 1978 - 30 September 1979	
	6. PERFORMING ORG. REPORT NUMBER R-1330	
7. AUTHOR(s) D. Das, K. Kumar, E. Wettstein, J. Wollam	8. CONTRACT OR GRANT NUMBER(s) N00014-77-C-0388	
9. PERFORMING ORGANIZATION NAME AND ADDRESS The Charles Stark Draper Laboratory, Inc. 555 Technology Square Cambridge, Massachusetts 02139	10. PROGRAM ELEMENT, PROJECT, TASK AREA & WORK UNIT NUMBERS	
11. CONTROLLING OFFICE NAME AND ADDRESS Office of Naval Research Department of the Navy 800 N. Quincy Street, Arlington, Virginia 22217	12. REPORT DATE October 1979	
	13. NUMBER OF PAGES 62	
14. MONITORING AGENCY NAME & ADDRESS (if different from Controlling Office) Office of Naval Research 666 Summer Street Boston, Massachusetts 02210	15. SECURITY CLASS. (of this report) Unclassified	
	15a. DECLASSIFICATION/DOWNGRADING SCHEDULE	
16. DISTRIBUTION STATEMENT (of this Report) Approved for Public Release, Distribution Unlimited		
17. DISTRIBUTION STATEMENT (of the abstract entered in Block 20, if different from Report)		
18. SUPPLEMENTARY NOTES		
19. KEY WORDS (Continue on reverse side if necessary and identify by block number) Arc Plasma                      Ion Implantation Beryllium                        Reactive Diffusion Boron                              CVD		
20. ABSTRACT (Continue on reverse side if necessary and identify by block number) The purpose of this program is to produce an adherent, low friction and wear resistant coating on a beryllium surface by in-situ formation of boride or borides of beryllium, with this goal being pursued via two distinct avenues of approach, i.e.; diffusion, and ion implantation. This report covers a period of roughly one year since October 1978. In the portion of the work which features diffusion from a solid boron source, we have now determined that the cause of earlier failures in producing bonded boride to beryllium substrates was due to formation of an oxide layer at the interface. Other significant accomplishments in the study of reactive diffusion process during this period are:		

7512F376



R-1330

MATERIALS RESEARCH FOR ADVANCED  
INERTIAL INSTRUMENTATION

TASK 2: GAS BEARING MATERIAL DEVELOPMENT  
BY SURFACE MODIFICATION OF  
BERYLLIUM

TECHNICAL REPORT  
FOR THE PERIOD  
1 OCTOBER 1978 TO 30 SEPTEMBER 1979

By

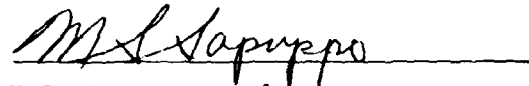
D. Das, K. Kumar, E. Wettstein, J. Wollam

Prepared for the Office of Naval Research,  
Department of the Navy, under Contract  
N00014-77-C-0388.

Approved for public release; distribution  
unlimited.

Permission is granted the U.S. Government  
to reproduce this paper in whole or in part.

Approved:



M.S. Sapuppo, Head  
Component Development Department

The Charles Stark Draper Laboratory, Inc.  
Cambridge, Massachusetts 02139

#### ACKNOWLEDGEMENT

This report was prepared by The Charles Stark Draper Laboratory, Inc. under Contract N00014-77-C-0388 with the Office of Naval Research of the Department of the Navy, with Dr. F.S. Gardner of ONR, Boston, serving as Scientific Officer.

The authors wish to express appreciation to the MIT Materials Science and Engineering Center for Auger spectroscopic analytical work performed by Drs. A. Garrat-Reed and R. Sorensen.

Publication of this report does not constitute approval by the U.S. Navy of the findings or conclusions contained herein. It is published for the exchange and stimulation of ideas.

TABLE OF CONTENTS

<u>Section</u>		<u>Page</u>
1	INTRODUCTION . . . . .	1
	1.1 Property Requirements . . . . .	2
	1.2 Limitations of Present Technology . . . . .	4
	1.3 Present Approach. . . . .	5
2	BERYLLIUM-BORON DIFFUSION EXPERIMENTS. . . . .	7
	2.1 Previous Work . . . . .	7
	2.2 Present Work. . . . .	8
	2.3 CVD . . . . .	16
	2.4 Experimental. . . . .	18
	2.5 Hardness Measurements . . . . .	34
	2.6 Conclusions . . . . .	38
3	BERYLLIUM BORIDING BY ION IMPLANTATION . . . . .	41
	3.1 Background . . . . .	41
	3.2 Progress Prior to This Reporting Period . . . . .	42
	3.3 Objectives . . . . .	43
	3.4 Progress in Fiscal Year 1979 . . . . .	44
	3.5 Other Progress and Preparation . . . . .	50
	3.6 Direction of Future Work . . . . .	53
	REFERENCES . . . . .	55

LIST OF FIGURES

<u>Figure</u>	<u>Page</u>
1 Boron side of a diffusion couple of amorphous boron powder hot pressed at 1000°C for 24 hours on a Be disc (magnification 500 ×) . . . . .	10
2-1 Diffusion interface, focused on the beryllium side. . . . .	11
2 Diffusion interface, focused on the boron side. . . . .	11
3 Schematic sketch of plasma-spray process . . . . .	12
4 Chemical vapor deposition system. . . . .	17
5 Color macrophotographs of CVD coatings by $BCL_3 + H_2$ gas (magnification 8 ×). (a) Earlier sample (#39) with chipped edges, and (b) more uniformly coated recent sample (#67) . . . . .	21
6 Slightly polished surface of an earlier sample (#39) which was CVD-treated to produce a red coating. Two different shades of pink appear distinctly different in black and white reproduction (magnification 500 ×). . . . .	22
7 The microstructure of a recently prepared CVD sample surface photographed in as-coated condition (magnification 500 ×) . . . . .	23

LIST OF FIGURES (Continued)

<u>Figure</u>		<u>Page</u>
8	20:1 slant cut to reveal the depth profile of a CVD sample similar to sample shown in Figure 6. (a) mag. 200 × shows entire thickness of CVD layer. (b) mag. 500 × shows the pink layer with two shades of pink . . . . .	25
9	Auger scans of sample #38 at various stages during sputter removal of the boride film. (a) before sputtering, (b) after 10 minutes of sputtering, (c) midway through sputtering and (d) after 64 minutes of sputtering . . . . .	27
10	SEM photograph looking down on a piece of spalled film from sample #64 (magnification 500 ×) . . . . .	29
11	Chemical composition of CVD layer, off sample #64 shown in Figure 10, shown as a function of sputtering time. (a) side away from Be-B interface, (b) side facing the Be substrate . . . . .	30
12	Auger spectra of the CVD layer at the end of sputtering. (a) corresponds to Figure 11(a), (b) corresponds to Figure 11(b) . . . . .	32
13	Sputter-deposited boron on a sputter-cleaned Be surface. The boron film has spalled off from the Be surface in the light area (magnification 8 ×). . . . .	33
14	Micrographs at 200 × of the light and dark areas of sample in Figure 13. (a) boron film in dark area is not continuous, showing exposed areas of Be, (b) light area shows patches where boron did stick well . . . . .	33
15	Auger spectra of boron sputter-coated Be after sputter cleaning. (a) boron coating, (b) areas where the coating had peeled off . . . . .	35

LIST OF FIGURES (Continued)

<u>Figure</u>		<u>Page</u>
16	Load vs. Knoop hardness values of surfaces of annealed beryllium and two boride beryllium surfaces by CVD . . . . .	36
17	Load vs. Knoop hardness values of the surfaces on sputter-coated Be surface with 0.3 $\mu$ B. (a) as sputter deposited, (b) after a heat treatment of 1000 $^{\circ}$ C for 15 minutes . . . . .	37
18	I-400 beryllium with 60 <sup>a</sup> /o boron implantation . . . . .	49
19	I-400 beryllium with 40 <sup>a</sup> /o boron implantation . . . . .	51
20	Direct implantation-degree of completion . . . . .	54

LIST OF TABLES

<u>Table</u>		<u>Page</u>
1	Materials and process options considered for bearing fabrication . . . . .	2
2	Knoop hardness, 3/8 inch discs implanted in low current machine . . . . .	47
3	Knoop hardness, 3/4 inch discs implanted in high current machine, as implanted . . . . .	52

SECTION 1  
INTRODUCTION

In the construction of gyroscopic inertial instruments, the purely structural requirements can be met through the use of instrument-grade beryllium, but gas-bearing surfaces require higher hardness and greater wear resistance than beryllium offers. This conflict has been solved in past and present instrument designs in a variety of ways, but operational discrepancies persist and a better solution is required. This task addresses this problem through materials research directed toward developing new materials and processes for this application.

The various types of materials and process options that have been investigated at The Charles Stark Draper Laboratory, Inc. (CSDL) and several other similar laboratories are shown in Table 1.<sup>(1,2,3,4)\*</sup> Initial attempts at CSDL were directed at fabricating entire gas bearings out of a solid piece of ceramic. Fabrication was accomplished by sintering and hot pressing techniques. Several difficulties were encountered in machining these materials, making the process expensive and time consuming. Additionally, the values of thermal expansion and thermal conductivity for these ceramics were very low.

The subsequent rationale developed to solve these problems envisioned the use of two different materials. One material was to form the structural member and satisfy bulk property requirements and

---

\* Superscript numerals refer to similarly numbered references in the List of References.

Table 1. Materials and process options considered for bearing fabrication

MATERIAL	PROCESS	PROBLEMS ENCOUNTERED
SOLID CERAMIC	SINTERING AND HOT PRESSING	DIFFICULT TO MACHINE PHYSICAL INCOMPATIBILITY  LOW THERMAL EXPANSION  POOR THERMAL CONDUCTIVITY
HARD COATINGS	PLASMA SPRAYING (THICK)	POROSITY, ADHESION, COHESION, PLUS ABOVE
	SPUTTERING (THIN)	ADHESION, COMPOSITION, STRUCTURE, MORE TOLERABLE THAN ABOVE BECAUSE OF THINNESS OF COATING
MODIFIED SURFACE	CASE HARDENING BY ALLOYING OF THE SURFACE	NONE OF THE ABOVE PERCEIVED

the other was to be deposited as a coating to yield a low-friction, wear-resistant surface. Therefore, a decision was made to investigate both thick and thin hard coatings on beryllium as the substrate. Since the structure of the instruments is made largely of beryllium, this material appears most suited for bulk property requirements. Of the several properties that are required in gas-bearing materials, the most important ones are listed below. The classification is divided, per the rationale discussed above, into bulk and surface properties, to underline the need for a composite, since no single material is expected to meet all of the stated property requirements.

#### 1.1 Property Requirements

The following properties are considered important for evaluating gas bearings:

#### 1.1.1 Bulk Properties

- (1) High thermal conductivity to avoid temperature gradients;
- (2) Nonmagnetic to eliminate interference with electromagnetic circuitry;
- (3) Thermal expansion compatibility with other structural members; and
- (4) Finishable to accurate tolerances of better than 1 micro-inch.

#### 1.1.2 Surface Characteristics

- (1) Low coefficient of friction for minimum bearing starting torque;
- (2) High resistance to wear from sliding, erosion, and impact for extended bearing life and improved performance; and
- (3) Zero surface porosity for maximum gas-bearing stiffness.

For these different reasons, as well as the availability of new coating processes like plasma spraying and sputtering, various films of ceramic materials have been fabricated and studied. The thickness of plasma-sprayed deposits currently in use is a few thousandths of an inch. The thickness of sputtered deposits that have been investigated is smaller than these by about two orders of magnitude. (Hence, the terminology "thick film" for sprayed deposits and "thin film" for sputtered deposits in Table 1). Examples of these processes are the plasma-sprayed chromium oxide and aluminum oxide coating now in use with some designs and the sputter deposited tungsten carbide and titanium carbide coatings that have been subjects of some development activity.

## 1.2 Limitations of Present Technology

The one feature common to both sprayed and sputtered coatings is the difference in physical properties between the coating and the substrate. While this may be somewhat tolerable in thin films produced by sputtering, thicker films made by spraying are susceptible to failure from imperfect match of expansion coefficients at the coating-substrate interface. To reduce stresses that result from differences in expansion coefficients, spraying is generally conducted at lower spray temperatures. However, this adversely affects interparticle cohesion strength, and results in pull-outs during polishing and lapping operations and generation of wear debris in active service. The clearance between the mating parts of a gas bearing is only about 50 micro-inches so that even the mildest form of wear (mildest by conventional standards) can prove to be intolerable in bearing applications.

A more severe problem that has been found in sprayed deposits is the presence of interconnecting porous structures in the coating. The effect of this interconnected porosity is to provide a shunt path for gas flow such that the hydrodynamic pressure rise is attenuated from that attainable with a nonporous coating.<sup>(5)</sup> This, in turn, causes a lower load capacity and stiffness for the gas bearing. In addition to this most severe effect, the porosity at the surface results in effectively increasing the bearing gap beyond the physical (design) clearance. Furthermore, although machining problems in sprayed deposits are less than those for sintered products (because parts are sprayed close to final size), they are nevertheless present albeit to a lesser degree on a small scale.

The adhesion of the coating to the substrate is an important consideration in wear performance. The forces that give rise to adhesion in films made from both these processes can be both mechanical and chemical in nature. The adhesion observed for deposits fabricated using the arc-plasma technology is generally found to be influenced by mechanical interlocking of the film on the external features of a

substrate. However, in both cases, chemical forces frequently give rise to stronger interfacial bonds. This type of bond is often termed a metallurgical or a diffusion bond. In chemically-compatible coating-substrate systems, the adhesion strength can be increased by depositing films at elevated temperatures (as in chemical vapor deposition or in physical deposition by sputtering or spraying) or by subjecting the substrate-coating composite to high temperatures. The former approach can result in a compressive state of the ceramic deposit at operating temperatures, whereas the latter can result in cracking of the deposit because of a tensile nature of the stress that will act on the ceramic coating upon heating. Ceramic materials generally behave well under a mild compressive loading. Poor adhesion has been the biggest problem with sputtered ceramic coatings formed on beryllium substrates.<sup>(4)</sup> Sputter deposited films have also shown large deviations from stoichiometric composition and the presence of undesirable microstructures. Depending on the conditions that are employed during fabrication, the structure of sputtered films could be either amorphous or crystalline. Columnar growth structures with poor interparticle bonding are frequently encountered in sputter deposits.

### 1.3 Present Approach

As shown in Table 1, the remaining process option, the one having the most potential for a successful gas bearing material, is case hardening. The focus of this task is to perform the necessary materials research to allow the development of a fabrication process for a precision, wear-resistant gas bearing in this area.

Efforts in the case hardening area have been going on for about two years and we expect to continue this activity. The approach is to form a hard beryllium-boride surface layer on a beryllium substrate. Two methods of producing this layer are being investigated: by reactive diffusion (as the reaction product of a boron layer deposited on a beryllium substrate) and by ion implantation of boron into beryllium.

All work related to reactive diffusion is being performed at CSDL. The ion implantation efforts are being carried on through the expertise and facilities of the U.S. Naval Research Laboratory. Analysis and evaluation in both reactive diffusion and ion implantation are performed at CSDL. Section 2 of this report describes the activities and status of beryllium-boron diffusion experiments, and Section 3 describes the efforts of beryllium boriding by ion implantation.

SECTION 2  
BERYLLIUM-BORON DIFFUSION EXPERIMENTS

2.1 Previous Work

The initial effort under this task was the high-temperature diffusion treatment of flat beryllium samples coated with a layer of boron. This activity was described in the first progress report<sup>(6)</sup> on this task and is summarized here.

- (1) Diffusion couples could not be formed under pressure at up to 1000°C using B and Be discs; there was no bonding or significant reaction;
- (2) Boron slurry-coated Be samples produced no bonding between Be and B at temperatures up to 1000°C;
- (3) Sputter-deposited boron coatings (0.5 and 1.0 micron thick) on a Be surface gave partially adherent layers which were subsequently heat treated. Heavier deposits (3.0 microns) using ion plating produced nonadherent coatings which were not heat treated; and
- (4) Be was heated in a boron vapor produced from a heated commercial mixture of  $B_4C$ , SiC and KF. An adherent coating was thought to have enough potential to warrant the construction of a conventional chemical vapor deposition apparatus in order to allow for suitable control of all process parameters.

## 2.2 Present Work

Subsequent to these experiments, considerable effort has been expended to understand the reason for nonadherence of borides to the beryllium surface. It is possible that any of the following could be the cause of nonadherence:

- (1) The type of boron (the high-temperature  $\beta$ -form, the low-temperature  $\gamma$ -form, or amorphous boron);
- (2) A barrier layer of beryllium oxide; and
- (3) Thermal expansion incompatibility between Be and the borides.

Item 1 would only have a bearing on the kinetics of the reactions; however, Item 2 would have a serious effect on both adherence and reactive diffusion. Item 3 may not be too significant a problem, if various compounds are formed resulting in a composition gradient. Composition gradients are known to result in strong bonding. Beryllium samples of the earlier experiments were analyzed and found to have heavy layers of beryllium oxide. A renewed effort was undertaken to form beryllium-boron couples devoid of oxide at the interface.

Beryllium and amorphous boron powder were used with a unique hot-pressing technique in an attempt to form a couple at 1000°C for 24 hours in an ultraclean high-vacuum environment. The reacted sample was composed of the following successive layers; Be, BeO, BeB<sub>2</sub>, BeB<sub>6</sub>, and B. The oxide layer on Be was again quite substantial. It is felt that the boron powder may have been the source of oxygen. On the boron side of the oxide layer, there were two distinct measurable layers of Be borides. The first was a comparatively thin metallic gray layer and the other a thick brick-red color layer. X-ray diffraction was used to identify the two layers as BeB<sub>2</sub> and BeB<sub>6</sub>, respectively. Obviously these high-boron, beryllium-boride compounds can be formed by reaction between Be and amorphous B at temperatures as low as 1000°C. The sample came apart at the interface between the layers BeO and BeB<sub>2</sub>.

A polished section of the B side is shown in Figure 1.  $\text{BeB}_2$  layer is about 10  $\mu$  thick which is comparatively dense. The next layer is rather porous and about 200  $\mu$  thick and is copper colored  $\text{BeB}_6$  with some  $\text{BeB}_2$  scattered throughout. The experiment cannot be called a true diffusion test. A temperature of 1000°C is too low to produce a dense compact of boron powder, resulting in a porous and loose compact on the Be Surface. Vapor pressure of beryllium being about  $2 \times 10^{-4}$  torr at the temperature, a large amount of the metal found its way through the pores in the loose boron on the surface. As the vapor moved through the boron particles the  $\text{BeB}_2$  and  $\text{BeB}_6$  compounds were formed. The movement of Be was therefore a vapor transport phenomenon rather than an atomic diffusion through the boron crystal lattice. Surface diffusion may also have played a role. Some time during the experiment a layer of BeO formed on the Be surface. Therefore the Be atoms must have diffused through the oxide layer before they moved by the vapor transport mechanism. This indicates that BeO is capable of dissolving excess Be in its crystal lattice. The absence of any boron on the Be side of the oxide layer indicates that boron is not soluble in BeO (at least up to a temperature of 1000°C) and thus could not diffuse through. Because of the clean separation at the BeO- $\text{BeB}_2$  interface, we conclude there there was no metallurgical bond between these two compounds.

A second approach to produce diffusion couples between Be and boron has succeeded in producing a well-bonded couple with no intervening BeO layer. A  $\beta$ -boron rod was buried in high-purity Be powder, followed by cold isostatic pressing and then hot isostatic pressing (HIP). HIP was carried out in an evacuated and sealed iron container which was thoroughly outgassed. The HIP operation was performed at an argon pressure of 15 Klb/in<sup>2</sup> at a temperature of 950°C for a period of two hours. The couple was removed from the container, and metallographic polishing revealed a bonded interface with a diffusion zone about 10 microns thick, and with what appear to be four layers within this zone. During polishing, because of the differences in hardness between the Be and B, the Be side was slightly depressed. Two separate microphotographs (Figures 2 and 2-1) were taken to bring out the interface between

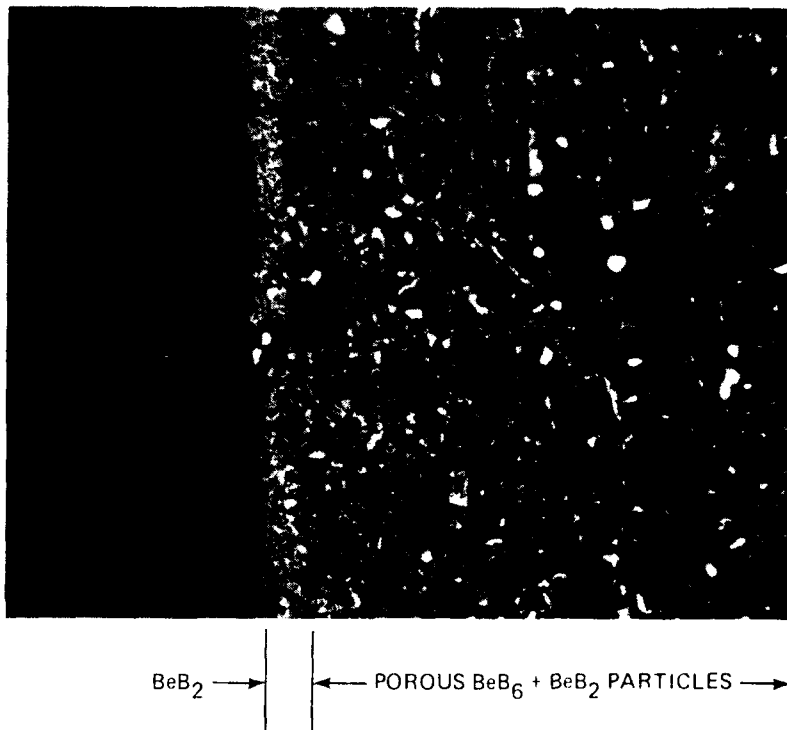


Figure 1. boron side of a diffusion couple of amorphous boron powder not pressed at  $1650^\circ\text{C}$  for 24 hours on a  $\text{BeB}_2$  disk (see caption on p. 8).

4/80 CD 19481

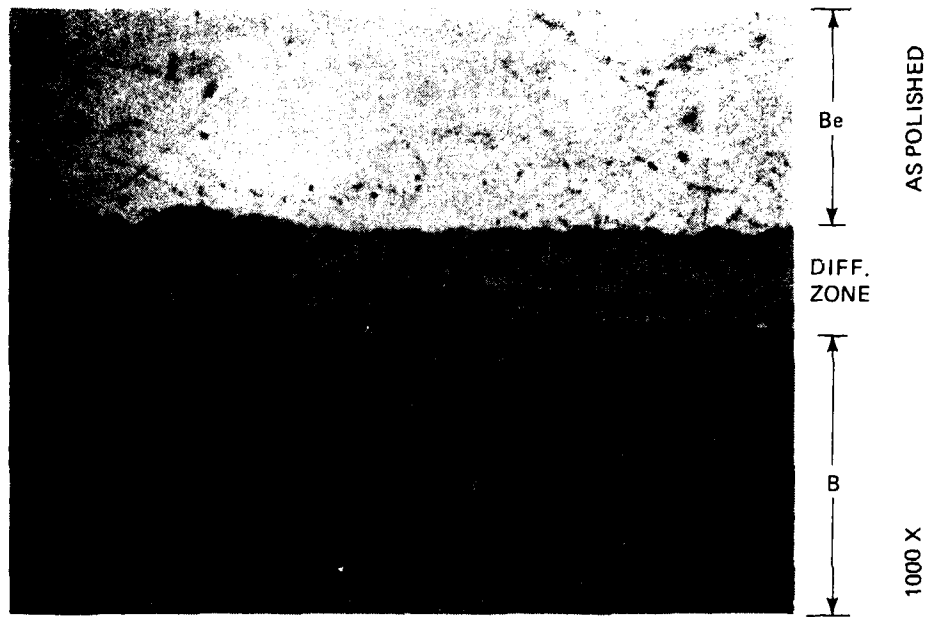


Figure 2-1. Diffusion interface, focused on the beryllium side.

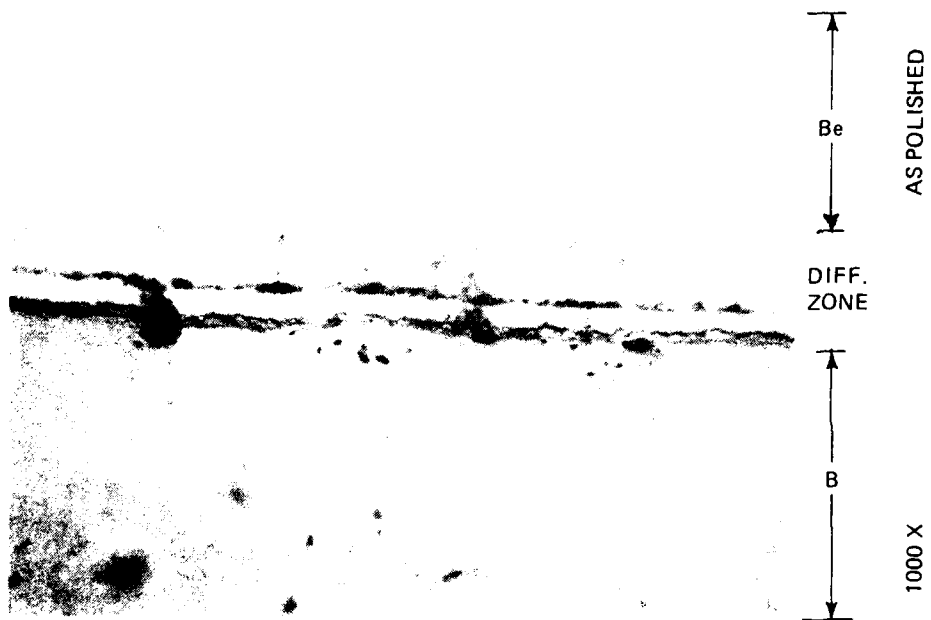
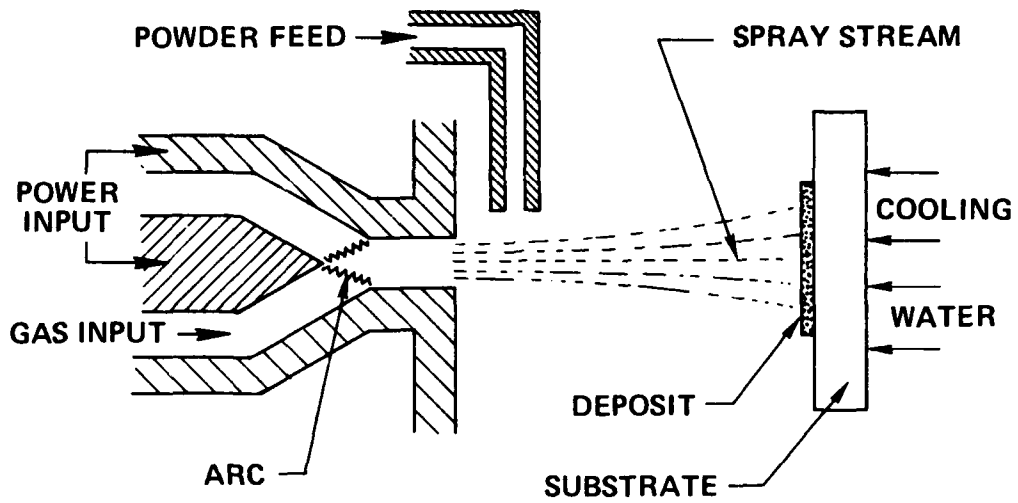


Figure 2. Diffusion interface, focused on the boron side.

4/80 CD 19482



10/77 12404 REV A 1/78

Figure 3. Schematic sketch of plasma-spray process.

Be and the diffusion zone between B and the diffusion zone. Both interfaces appear well bonded and this method appears to be a successful technique for producing Be-B diffusion couples. Auger microprobe analysis indicated one of the diffusion layers as  $\text{BeB}_6$ . The  $\text{BeB}_6$  layer gave a hardness value of 1400 VHN which is in itself encouraging as this is a suitable value for a gas bearing surface. With the development of HIP technique, the study of the growth kinetics of the various intermetallic compounds of Be and B boron may now proceed. We are now ready to start the study of diffusion kinetics of the system Be-B using both  $\beta$  and  $\gamma$  (lower temperature form) boron in a systematic manner. The diffusion couple produced initially was not considered adequate because of the irregular shape of the  $\beta$  boron sample used. The sample was produced mainly to determine the feasibility of HIP technique for fabrication of diffusion couple.

$\beta$ -boron is commercially available in small diameter rod form or irregular shaped pieces. Since the rod diameter (used in one initial preparation) is small, we have decided to use more massive irregular pieces. A number of such pieces of  $\beta$ -boron have been ground flat on one side in our machine shop. This would give us planar geometry when HIP bonded with Be powder for diffusion studies. Large pieces of solid  $\gamma$ -boron are not available commercially. However,  $\gamma$ -boron is important from our point of view, since the methods we will use for depositing boron on beryllium surface will most probably become  $\gamma$ -boron at the diffusion temperature of 900 to 1050°C, if not already in that form during deposition. Essentially pure boron can be prepared in an unusually large number of crystalline forms; however, most such polymorphs can be considered as due to extreme cases of nonstoichiometric boron compounds.<sup>(7)</sup> It is now well accepted that there are three established crystalline forms -  $\alpha$ -rhombohedral (low temperature form)<sup>(8)</sup>,  $\beta$ -rhombohedral (high temperature form)<sup>(9)</sup>, and  $\gamma$ -tetragonal (intermediate temperature form)<sup>(10, 11)</sup>. There is some doubt about the temperature ranges of stability for these various polymorphs. It is however safe to say that  $\beta$ -rhombohedral is stable from m.p. (approximately 2200°C)

down to 1500°C or even lower,  $\alpha$ -rhombohedral from 800 to 1100°C and  $\gamma$ -tetragonal from 1100 to perhaps 1300°C.<sup>(12)</sup> Of the three polymorphs,  $\beta$ -boron appears to be the most stable.  $\alpha$  and  $\gamma$  forms are developed possibly as a consequence of favorable growth kinetics, with a considerable overlap in their reported stability range. There has been no evidence of transformation from  $\alpha$  to  $\gamma$  form or vice versa.  $\alpha$  becomes very unstable above 1200°C, giving as yet unidentified structures finally changing to  $\beta$  form at 1500°C. This does not suggest that  $\alpha$  is stable to 1200°C. Instead it may just indicate a sluggish transformation. If boron is deposited on a reactive surface, in the temperature ranges where  $\alpha$  may form, the crystalline form is that of  $\gamma$ -boron, with no evidence of  $\alpha$ , even when the deposit is quite thick. In our CVD work because of the above facts we expect that the deposit is more likely to be  $\gamma$ -tetragonal rather than  $\alpha$ . A determination of the crystalline character has not been possible because the deposits are too thin for x-ray diffraction and they have mostly been converted to borides during deposition. Nevertheless it is important to determine if there is a difference in the diffusion kinetics of the systems Be- $\beta$ B and Be- $\gamma$ B.

Since solid  $\gamma$ -boron is not available commercially, we decided to try to prepare some solid pieces by arc-plasma spraying. For starting material we used commercially available 99% pure crystalline boron powder. The powder was designated as -100 mesh. To ensure maximum melting of the powder in the plasma spraying process, we decided to use particles less than 44 micron in size. We sieved the boron powder on a 325 mesh screen and found that more than 50% passed through. We used the minus fraction. X-ray diffraction of the powder gave a pattern which corresponded very well with published pattern of  $\beta$ -rhombohedral boron.

A schematic sketch of the arc-plasma spray process is shown in Figure 3.<sup>(13)</sup> The process consists of excitation of an inert gas plasma with a high intensity dc arc. The plasma exits through a nozzle and acquires high velocity. The powder to be deposited is introduced at

this stage into the plasma flame by means of an inert gas that serves as a carrier. The powder particles melt and form small molten spheres, which are propelled at sonic speed, and splashed and deposited on a water cooled substrate. The quenching of the deposit occurs in microseconds with usual cooling rate in the range of  $10^6$  degrees centigrade per second.

A mixture of argon and hydrogen was used to form the plasma. Argon was also used to form the ambient atmosphere in a waterjacketed, controlled environment chamber. The boron deposits were formed on a grooved, watercooled copper substrate with a 40 KW Metco 3MB plasma spray gun. A number of runs were made to produce deposits with thickness in the range of 2 to 3 mm. The samples were easily removed from the copper substrates by prying them loose with a knife blade. The surface in contact with the chilled copper had a slightly copper color which was easily removed by rubbing on a 600 grit polishing paper. X-ray diffractometer traces were made on both the copper cooled face and the side facing the plasma gun. The copper cooled side showed a  $\gamma$ -tetragonal pattern. One of the samples was then ground to a powder and an x-ray diffractometer pattern taken of the powder. This resulted in a pattern showing both  $\beta$  and  $\gamma$  lines. A rough estimate of this pattern showed that  $\beta$  and  $\gamma$  are about equal in amount in the powder.

These plasma sprayed samples, we feel, are going to be satisfactory for forming Be- $\gamma$ B diffusion couples if we concentrated our studies to the surface which was in contact with chilled copper. We decided to determine if the  $\gamma$ -B we had produced would be stable at diffusion study temperatures of 900 to 1050°C. We heat treated a piece at 1050°C in argon atmosphere for 24 hours. X-ray diffraction patterns of this sample gave identical patterns from both sides, as were obtained prior to the heat treatment, except perhaps a slight sharpening of the lines. Obviously the  $\gamma$ -B formed on the chilled copper surface would remain as  $\gamma$ -B during our diffusion treatments. The same sample was then given a heat treatment at 1700°C for 1 hour in a  $10^{-6}$  torr vacuum. The whole sample after the above treatment became completely  $\beta$ -rhombohedral boron.

At this time we have an adequate supply of both  $\beta$  and  $\gamma$  forms of boron in usable shape to produce necessary number of diffusion couples with beryllium by the HIP techniques. We plan to produce these couples in the near future.

### 2.3 CVD

Although the HIP technique has successfully produced bonded Be-B, it may not be a suitable method of producing hard boride surfaces on gas-bearing components. Chemical vapor deposition (CVD) is the most appealing alternate process because of its simplicity. The CVD of boron has been reported in the literature from two different types of gaseous sources: diborane ( $B_2H_6$  - a gas at room temperature)<sup>(14)</sup> and boron trihalide ( $BCl_3$ ,  $BBr_3$ , etc.) plus hydrogen.<sup>(10)</sup> Diborane decomposes to boron and hydrogen when heated, whereas  $BCl_3$  gas reacts at high temperatures with hydrogen, producing boron and HCl gas. In either case, free boron is made to form on a heated Be surface where it is expected to react and form the intermetallic compounds.

In addition to the above gaseous CVD processes another process employing solid material and a gas phase transport catalyst<sup>(15)</sup> has been used successfully to produce boride coatings on titanium alloys. It is possible we may look into this process more thoroughly.

A CVD apparatus capable of employing either of the two processes described above, has been designed and built. A photograph of the system is shown in Figure 4. The sample to be coated is supported in the center of a 1-1/4 inch diameter quartz tube, and a spiral water-cooled copper coil is placed on the outside of the quartz tube where the sample is located. A high frequency Lepel power supply capable of producing 2 KW is connected to the copper coil for direct heating of the sample by induction. Vacuum tight flanges are provided on both ends of the quartz tube, for introduction of gas from one end and a vacuum pump and exhaust tubings on the other end. A quartz window on the gas entry flange allows temperature monitoring with an optical

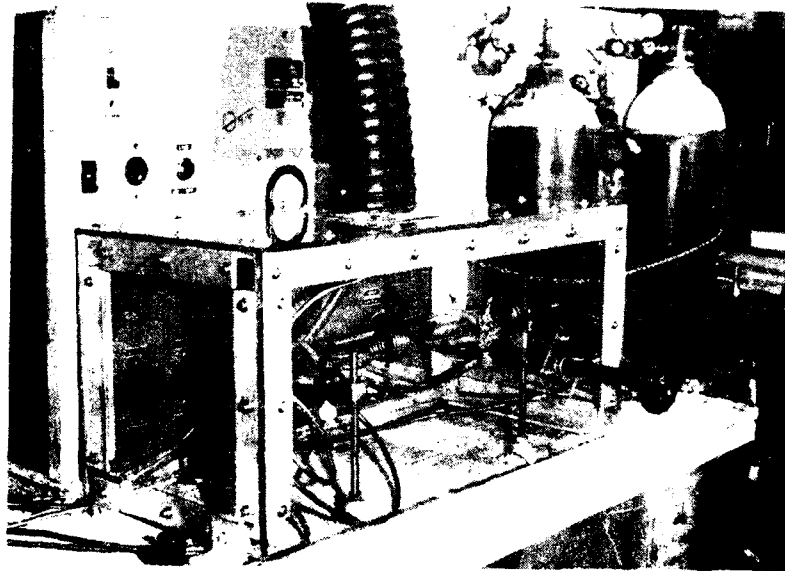


Figure 4. Chemical vapor deposition system.

4-80 CD 19483

pyrometer. A sturdy plexiglass box with an aluminum frame provides safety, and also functions as a hood. It is connected at the top to an exhaust system with a measured capacity of 100 cfm by means of a flexible 5-inch pipe. A small clearance between the table top and the bottom of the box allows air-flow into the hood. The spent gas from the quartz tube is exhausted directly into the flexible exhaust pipe, as also the exhaust from the vacuum pump.

The CVD system has been operational for several months and a substantial number of deposition experiments have been performed using both diborane and  $\text{BCl}_3$  and  $\text{H}_2$  gases. A limited degree of success has been achieved by both the processes for formation of adherent boride films on heated beryllium substrates. Films produced so far have been rather thin of the order of one micron. We have encountered some problems of cracking and spalling in trying to produce heavier films. At this stage we are not sure whether heavier films would be necessary. However, we will continue our experimental studies to be able to produce heavier films. In the meantime, the thin films are giving us high integrity coating of good uniformity, fairly high hardness and strong adherence.

#### 2.4 Experimental

The procedure for producing a CVD film on Be surface is described in what follows. The sample in the form of a circular disc (0.5 inch diameter X 1/8 inch thick) or a rectangular piece about 1/8 inch thick and similar cross sectional area as the circular disc, with metallographically polished surface was placed in the quartz tube within the area surrounded by the induction heater coil. A stainless steel wire device with two prongs inserted into two tiny holes drilled into the Be sample from the edge supported it without allowing it to touch the walls of the quartz tube. In the initial experiments the axis of the sample discs were made nearly to coincide with the quartz tube axis, in order to make one of the faces of the sample lie on the direct path of the incoming

CVD gas. In later experiments the samples were oriented with an edge facing the gas flow. This has resulted in more uniform coating of the entire sample.

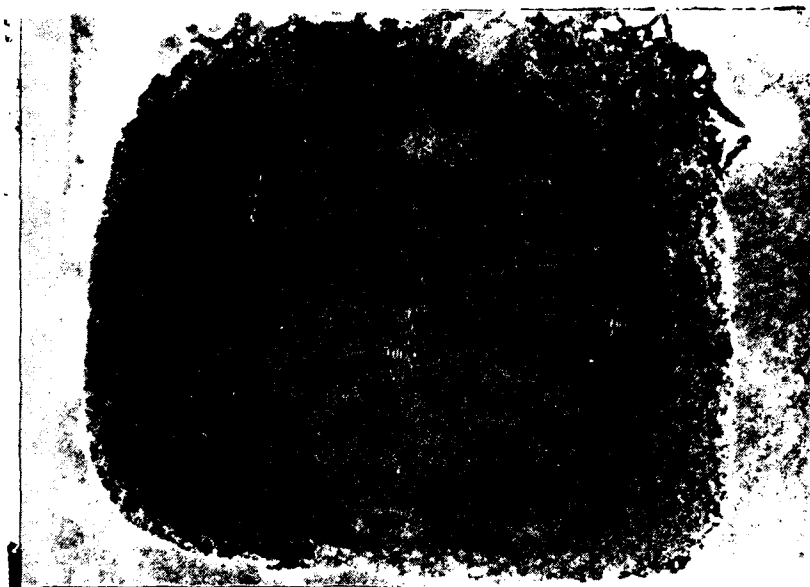
The general procedure for the CVD has been to purge the tube by repeated evacuation and filling of the tube with either argon or hydrogen followed by heating the sample to the deposition temperature for 15 minutes in the flowing gas. No visible differences were noticed in the characteristics of the deposits whether the initial heating was done in hydrogen or argon atmosphere. Therefore in all of the runs after the first few the initial heating was done in argon. Following the initial heating the CVD gas was introduced at a given flow rate for a period of time, and then the CVD gas flow was cut off and sample was slowly cooled to room temperature in approximately two hours or so. In other cases the samples were cooled quickly by turning off the power to the induction coil after the desired CVD treatment.

All the gases used have been 99.999% pure. The CVD gases were premixed by the vendor. The diborane source was a premixed gas composed of 99.9% pure argon and 0.1%  $B_2H_6$ . The trichloride gas was composed of 70% argon, 29%  $H_2$  and 1%  $BCl_3$ . The chemical reactions in the two processes are as follows:  $B_2H_6$  decomposes to boron and hydrogen at elevated temperatures. The freshly formed boron on the hot beryllium surface would then react with beryllium to form the borides. The morphology of the coating would depend on the rate of deposition of boron and the diffusion kinetics of the system Be-B, and the time and temperature of the experimental duration. In the case of the trichloride CVD gas system the  $BCl_3$  reacts with  $H_2$  at elevated temperature to form elemental boron and HCl gas. Once again the elemental boron on the hot beryllium surface would form boride or borides according to the time-temperature parameters.

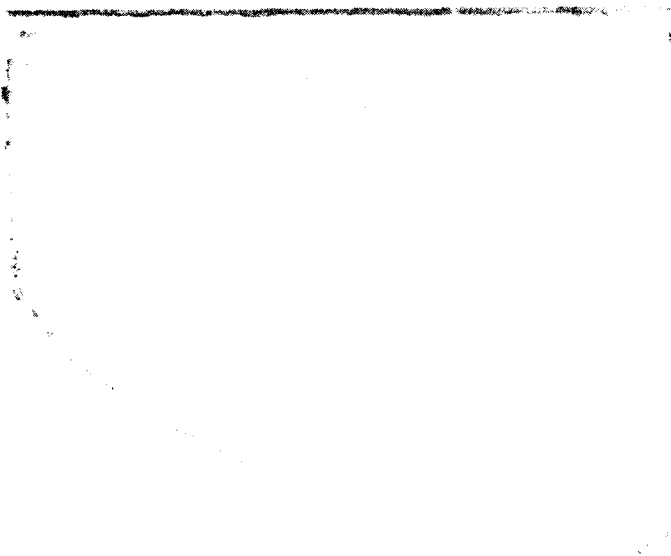
The initial deposition experiments were carried out using the diborane gas. With diborane as the boron vapor source, the visible decomposition starts in front of the heated substrate (obviously at

quite a low temperature) and boron deposits on the Be surface with very low integrity. There was a lack of cohesion between the boron atoms and this was one of the reasons that boron tended to flake off from the Be surface. However, some samples with partial adherence with what appear to be bonds of a chemical nature have been produced.

In an attempt to gain an early appraisal of the potential of CVD using boron trichloride as a boron vapor source, the diborane experiments were interrupted, and the apparatus modified to employ this source. The chemical reaction between  $\text{BCl}_3$  and  $\text{H}_2$  is a higher temperature process (minimum temperature of  $800^\circ\text{C}$ ) than diborane deposition and the reaction is believed to occur only on the heated beryllium substrate enhancing the chance of reaction between the freshly-formed free boron atoms and the Be surface. First experiments yielded adherent, hard (resistant to polishing) deposition layers. The coatings usually chipped off around the edges, but in the middle the coating was found to be strongly adherent to the substrate and with a fair degree of hardness. In one recent set of experiments, we have been able to produce completely coated samples, with strongly adherent uniform films of good hardness values. Example of coatings of the two types are shown in Figures 5(a) and 5(b) in macro color photographs to show the pink colors of the coatings. Whenever the color of the coatings have gray or gray-blue appearance the deposits are nonadherent and tend to flake off. The oxygen content of these latter deposits are high and caused most probably by air leaks (real or virtual). Extreme care in cleaning of the quartz tube including baking it out prior to deposition results in adherent pink color deposits. Although the appearance of the surface is uniform in color, under large magnification the surfaces appear to be composed of two phases - a light pink phase and a darker pink one (see Figure 6). The two phases appear in relief, due perhaps to the effect of sandblasting the surface prior to CVD treatment. For comparison we are presenting the photomicrograph of a recently CVD treated sample in as-coated condition (see Figure 7).



(a)



(b)

4/80 CD 19484

Figure 5. Color macrophotographs of 2000-20000 Å of  $H_2$  gas  
(magnification  $\times 5$ ). (a) Earlier sample (#66) with chipped  
edges, (b) more uniform water-cooled sample (#67).

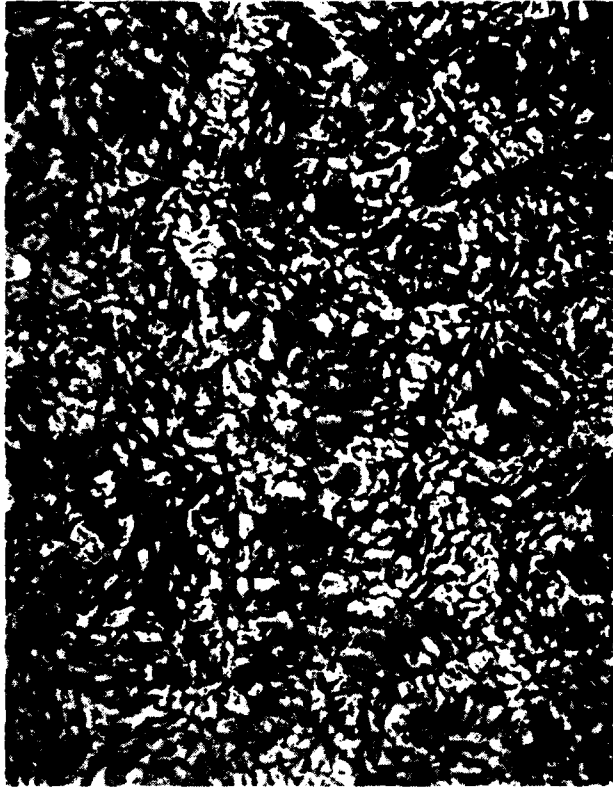


Figure 6. Slimely, whitish, center of same culture sample (#87) when was subjected to the same conditions as before. On different stages of growth, the color of the culture changes from pink and white to black. (Magnification: 100x)

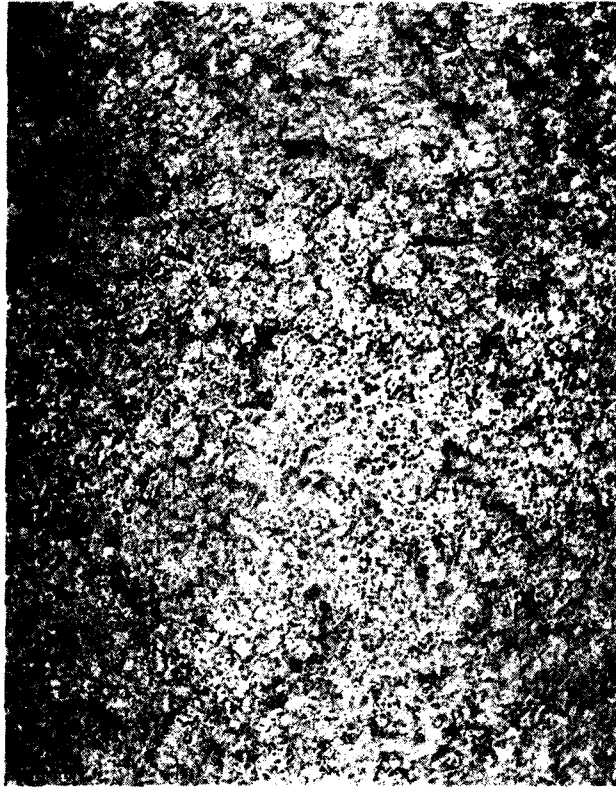
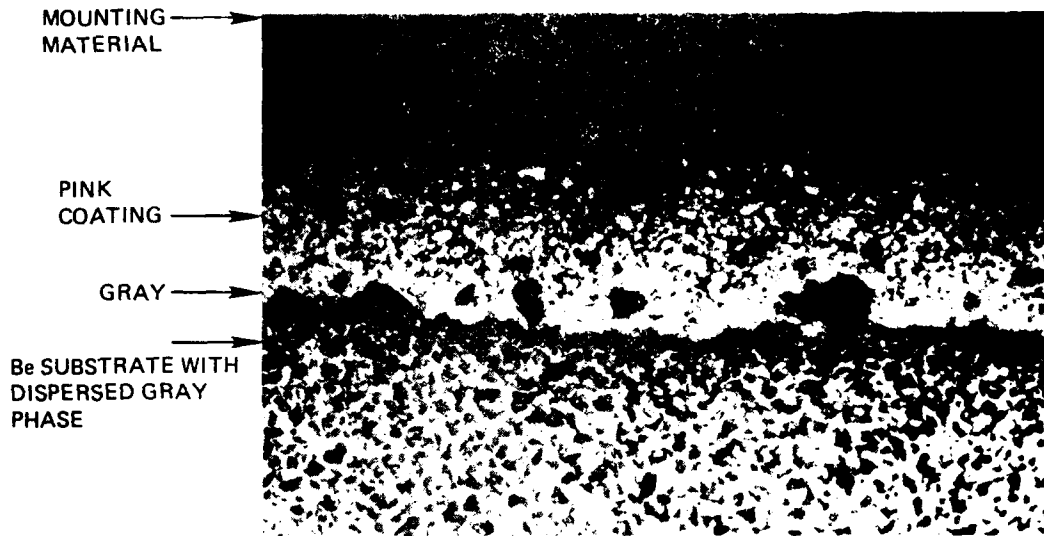


Figure 7. The microstructure of a recently prepared CVD sample surface (photomicrograph presented condition of magnification 500 x).

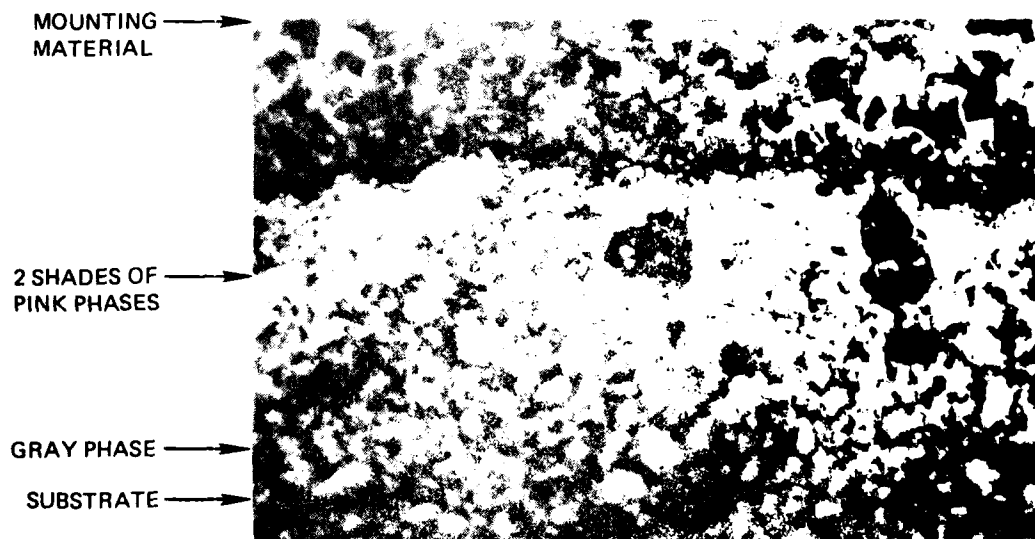
Because of our improved techniques the surface is much smoother, shiny pink and has a much finer grained appearance. In this case also there are two distinctly different shades of pink.

It would be very desirable to examine the extent of the penetration of boron into the beryllium substrate. Since the layer is usually less than a micron in thickness a normal cross section through the coating was not possible. We therefore prepared a sample section at a highly slanting angle to the surface which amplified the thickness of the layer by a factor of about 20x. In figures 8(a) and 8(b) the interface between the beryllium substrate and the CVD coating are shown in the magnifications of 200X and 500X. The voids in the pink layers are believed to be pullouts during the polishing operations.

Since the CVD coatings on beryllium formed thus far are in the range of less than a micron, x-ray diffraction identification was not possible. We have therefore carried out some Auger spectrographic analysis to obtain an idea of what we have formed on the beryllium surfaces by our CVD technique. Of course, Auger analysis gives only the elemental analysis. Some conclusions can be formed about the chemical state by combining the Auger results along with other known parameters. One has to recognize the fact also that the Auger spectrum gives information about only the very superficial layers of the surface, perhaps no more than just a few atomic layers because of the rather low energy of the incident electron beam which produces the Auger electrons. The spectra, however, are capable of giving quantitative information about the chemical composition of the surfaces being analyzed. The Auger machine we have been using at the Massachusetts Institute of Technology (MIT) has the capability of giving chemical analysis of material below the surface. This is achieved by sputtering off materials from the surface while the specimen is located within the specimen chamber and being analyzed. By continuously sputtering and monitoring the intensities of Auger spectral lines of various elements present in the film a chemistry depth-profile is determined.



(a)

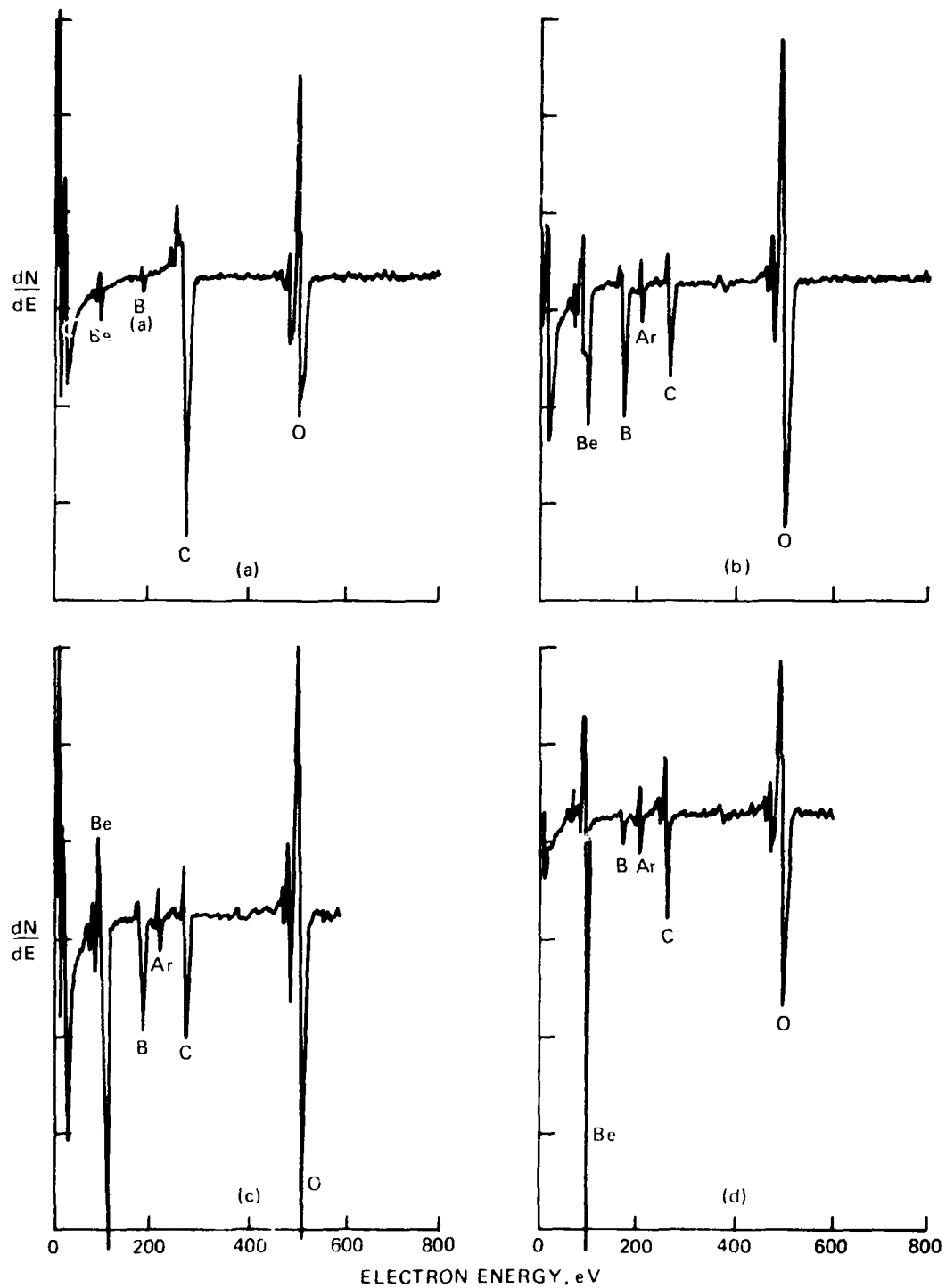


(b)

Figure 8. 20:1 slant cut through a Be sample similar to sample shown in Figure 7. (a) shows entire thickness of Be sample and (b) shows the pink layer with the same magnification.

We have carried out some Auger analysis and the technique appears to be very well suited for the evaluation of the CVD coatings we are studying. However, the Auger analysis will eventually have to be supplemented by crystallinity identification technique, such as glancing angle electron diffraction. As already mentioned, x-ray diffraction will possibly be of very little use in this area because of the low atomic weights of both beryllium and boron in addition to the extreme thinness of the films.

The Auger spectra of sample 38 are shown in Figure 9, the scans being taken at four different times while the coating was sputtered off. The total sputtering time was 64 minutes. Assuming a rate of sputtering between 100 and 200 Å/min, it would appear that the film thickness was in the vicinity of 1 micron. Before sputtering, Be and B peaks are barely visible under a dense layer showing C and O. Exposure to air and cleaning of the sample in acetone and alcohol might explain the abundance of C and O in the initial surface layers. All the scans on Figure 9 were taken with a voltage of 5 KV for the primary beam. This results in practically equal intensity of Be and B lines for equivalent amounts of the elements. Oxygen line intensity is approximately 5 times that of Be and B, while C gives twice the intensity for equal volumes of the elements. In analyzing the various scans shown in Figure 9 we should bear the above facts in mind; it is also reasonable to assume that whatever oxygen is seen on the surface after removal of the initial layers by sputtering must be in the form of BeO because of the temperature to which it was subjected during the CVD treatment. Using the above arguments, it appears that Figure 9(b) is composed of about equal amounts of BeO and a beryllium boride with a stoichiometry of  $\text{BeB}_2$ . The surface after about 30 minutes of sputtering is still composed of equal amount of BeO to boride. But the boride composition now appears to be that of  $\text{Be}_2\text{B}$ . At the end of sputter removal, the BeO amount has gone down substantially but during sputtering procedure it appears to attain a very reduced but constant



4/80 CD 19486

Figure 9. Auger scans of sample #38 at various stages during sputter removal of the boride film, (a) before sputtering, (b) after 10 minutes of sputtering, (c) midway through sputtering and (d) after 14 minutes of sputtering.

value. The value of carbon content may be due to the background in the Auger machine which utilizes oil pumps for its vacuum environment. Although the Auger scans indicate that the coating is composed of the compound  $\text{BeB}_2$ ,  $\text{Be}_2\text{B}$  and  $\text{BeO}$ , we will eventually have to pin down the real identity of the compounds by some diffraction technique. It is somewhat surprising that even with all the oxygen in the film, it still is highly adherent to the beryllium substrate as long as the film thickness is in the range of one micron or so.

Sample 64 was given similar treatment as sample 38 but was repeated four times in order to produce a much heavier film, without removing the sample from the CVD chamber until after the final run. The coating was beginning to crack and spall when it was brought out. It was noticed that the film had a dull grey color on the substrate side and copper colored on the side away from the interface. The film thickness was determined to be between 4 and 5 microns from an SEM picture taken edgewise of a piece of spalled film (see Figure 10).

We decided to do a thorough Auger depth profile analysis of the spalled film from sample 64. Two small pieces were mounted on an aluminum sheet (1 cm x 1 cm) using a silver cement with the copper color showing on one piece and the grey side showing on the other. Both pieces gave similar Auger spectrum prior to sputtering as in Figure 9(a). We then sputtered and continuously monitored the peak heights of the four elements during sputtering. The copper colored side was sputtered for 56 minutes and the grey side (facing the Be substrate) for about 30 minutes. These scanning data are shown in Figure 11. After about four minutes of sputtering on the copper color side oxygen went down to a very low concentration and remained constant. Be and B on the other hand increased and remained more or less constant at the ratio of about 1:1 (Figure 11(a)). Figure 11(b) shows the sputter-scan data on the grey side of the film. The oxygen concentration remained fairly high throughout at about 4 times the amount on the copper side of the film. Be concentration was found to be constant at



FILM THICKNESS

Figure 10. SEM photograph looking down on a piece of spalled film from sample #64 (magnification 500 ×).

4/80 CD 19487

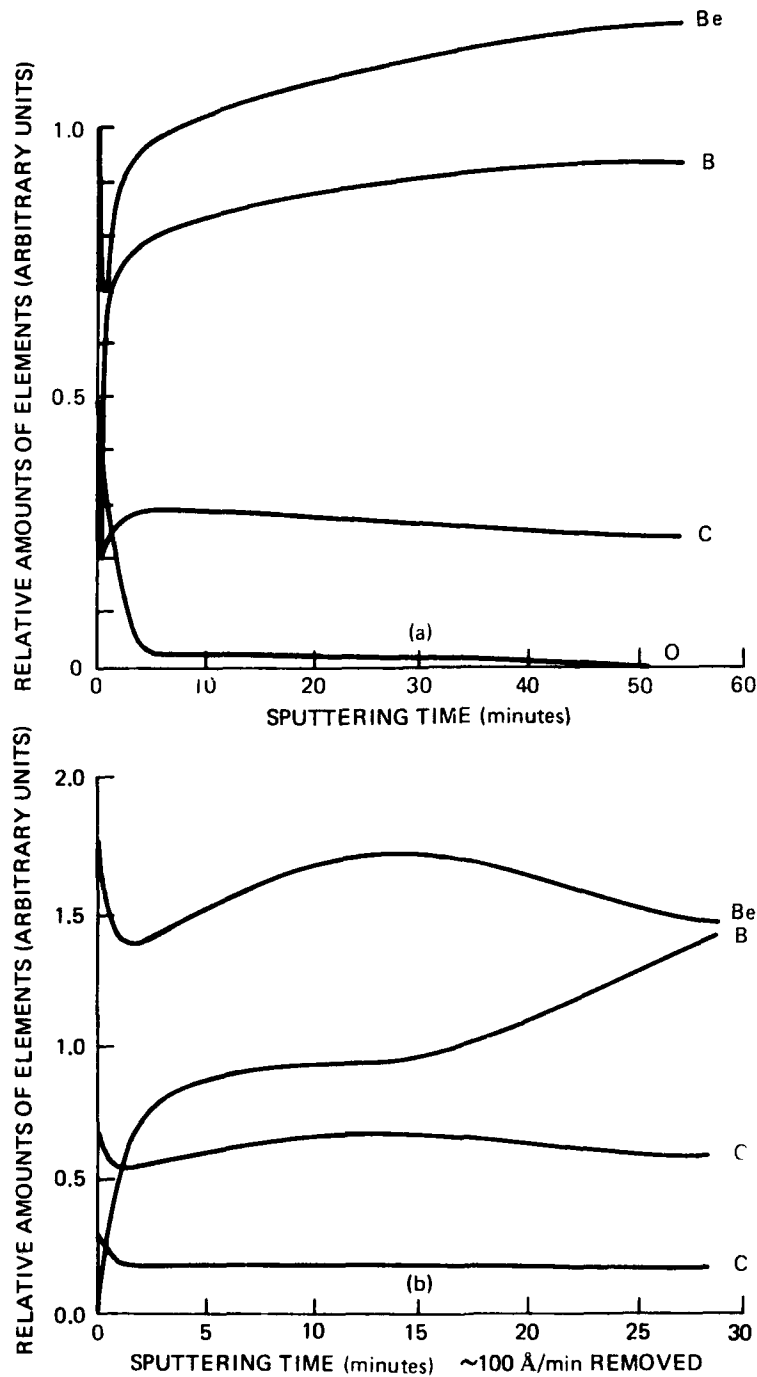
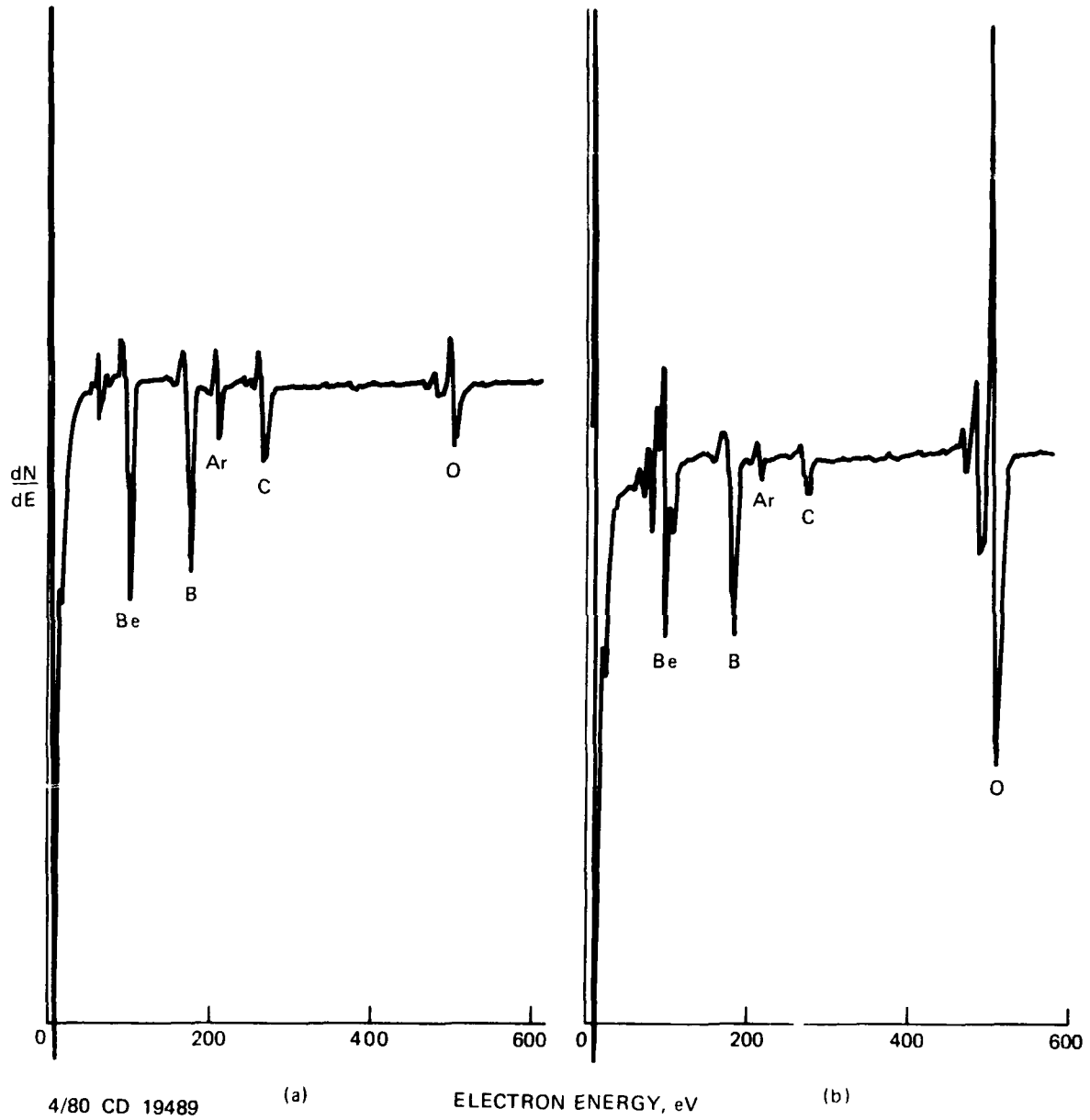


Figure 11. Chemical composition of CVD layer, off sample #64 shown in Figure 10, shown as a function of sputtering time. (a) side away from Be-B interface, (b) side facing the Be substrate.

4/80 CD 19488

about the same level as on the copper side. B was very low to start with but rose to a level about half that of Be for about 0.1  $\mu\text{m}$  (1000 angstroms). In the next 1500  $\text{\AA}$  B reached the equal level of concentration as Be. At the end of sputtering an Auger scan of each sample was taken, shown in Figure 12. The substrate side shows very large oxygen concentration, whereas the copper color side shows a very small oxygen peak. Allowing some Be to be in oxide form, it appears from Figure 12 that Be and B are in a stoichiometry of 1:1. The only way that could happen is if this rather substantial layer (about 3.5  $\mu\text{m}$ ) could be a region where the two compounds  $\text{Be}_2\text{B}$  and  $\text{BeB}_2$  coexisted. The evidence we have at this time is not conclusive.

It begins to appear more conclusively that oxygen is hampering the formation and adherence of the boride layers. Very thin films are quite adherent. But so far we had difficulty in forming films of thickness around 4 or more microns. We thought we could perhaps get around that problem by sputter depositing a thin boron film on sputter cleaned beryllium surface and then proceed with CVD technique to build up the thickness and thus produce boron-rich beryllium borides. However, sputter deposition technique has not produced satisfactory results. Sputtered boron films on sputter cleaned surfaces tended to peel off even for thicknesses as low as 0.3  $\mu\text{m}$ . A macrophotograph of a sample with 0.3  $\mu$  thick deposit is shown in Figure 13. The dark area on larger magnification (Figure 14(a)) shows small patches within the film that have spalled off leaving bare beryllium. In the light area - Figure 14(b) - boron adhered only to some selected areas. Auger scans were taken of the dark boron areas and light Be areas after removing about 200 angstroms by sputter cleaning the surfaces. The Be surface still shows heavy amounts of oxygen with no trace of boron. (Figure 15(b)). The dark areas show no beryllium and oxygen level is much smaller. (Figure 15(a)).



4/80 CD 19489 (a) ELECTRON ENERGY, eV (b)

Figure 12. Auger spectra of the CVD layer at the end of sputtering. (a) corresponds to Figure 11(a), (b) corresponds to Figure 11(b).

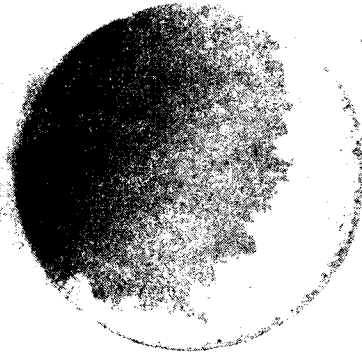
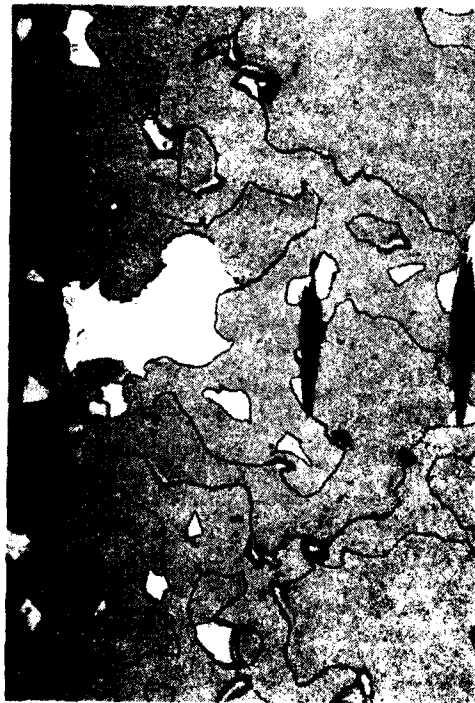


Figure 13. Sputter-deposited boron on a sputter-cleaned Be surface. The boron film has spalled off from the Be surface in the light area (magnification 8 $\times$ ).



(a) (b)



Figure 14. Micrographs at 200 $\times$  of the light and dark areas of sample in Figure 13. (a) Boron film in dark area is not continuous, showing exposed areas of Be; (b) light area shows surface where boron film did not well.

## 2.5 Hardness Measurements

True hardness values are practically impossible to determine of a material when it occurs in a very thin film form on a comparatively soft material. It is especially so if the depth of penetration of the indenter is equal to or larger than the thickness of the film. However, one could take a number of hardness measurements using various indenting loads ranging all the way from very large to quite small. If the film is composed of a hard material and the substrate is soft, measured hardness values would increase as the indentation load is decreased. This is because the lower the load, the less is the penetration into the soft substrate, and therefore more of the indentation load is supported by the harder material. The result would consequently be a larger hardness value obtained for the composite, but still lower than the true hardness value of the film.

Varying load hardness measurements were carried out on following samples: (1) annealed beryllium; (2) two (CVD-coated samples - numbers 37 and 62; (3) boron sputter deposited in as-deposited and heat treated condition. The results of these measurements are shown in Figures 16 and 17. The CVD samples appear to show much higher hardness than the virgin beryllium surface. Exact values of the coating can only be a conjecture at this time, but they are definitely comparable to the hardness values of plasma-sprayed surfaces of presently used gyro gas bearings. Figure 17 shows the measured hardness values on sputter-coated sample, in as-sputtered and after heat treatment. In as-sputtered condition, we measured a value of 3100 KHN on a boron coated area, which is excellent. However, on a short heat treatment, the coating became very crumbly and the hardness values went down to the level of pure beryllium. Although the boron coating by sputtering on the beryllium surface has very good hardness, it is not considered satisfactory because the deposits are patchy and rather nonadherent. Adherence could not be produced by heat treatment because of thermal expansion mismatch, resulting in a crumbly surface.

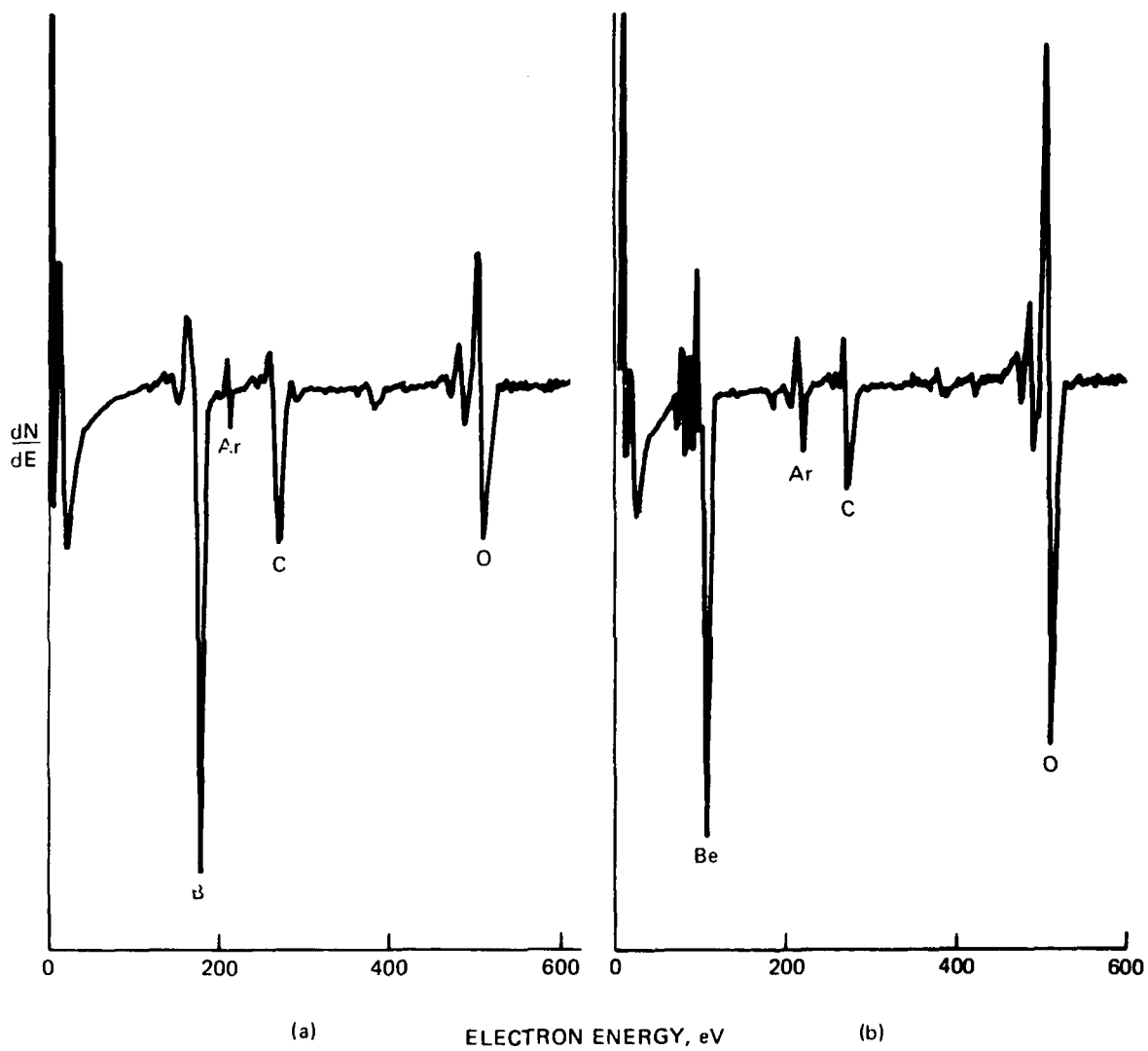
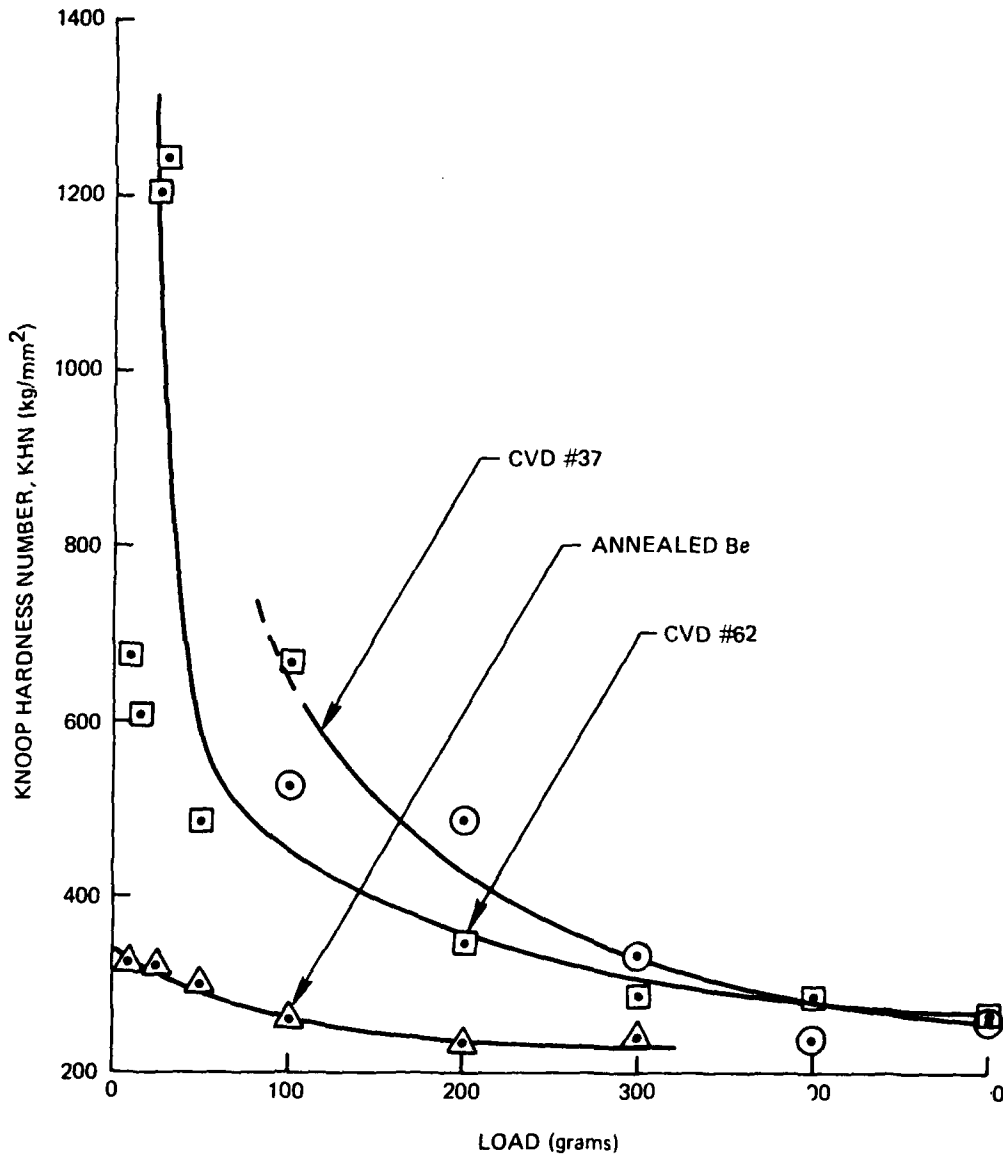
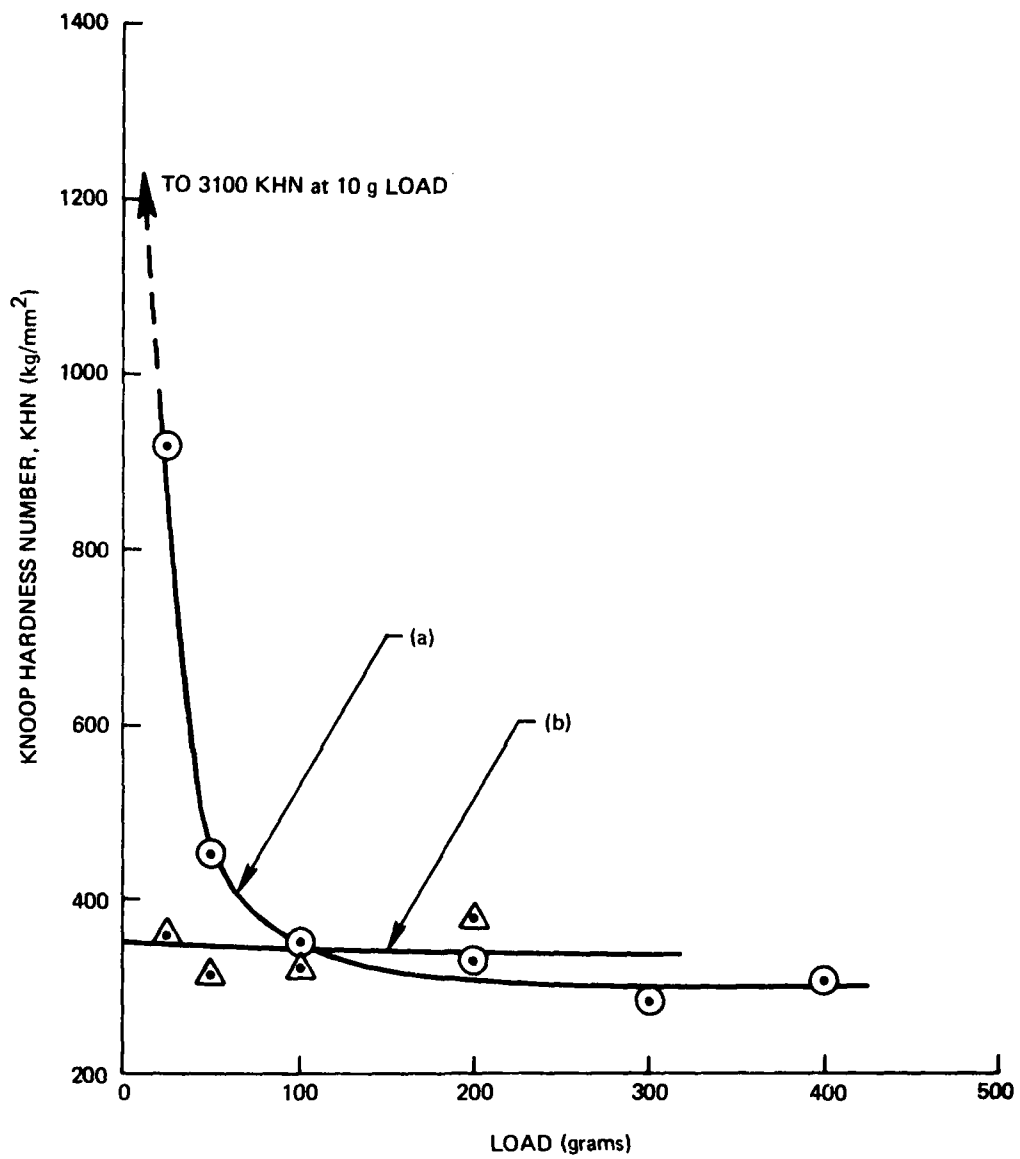


Figure 15. Auger spectra of boron sputter-coated Be after sputter cleaning. (a) boron coating, (b) areas where the coating had peeled off.



4/80 CD 19490

Figure 16. Load vs. Knoop hardness values of surfaces of annealed beryllium and two borided beryllium surfaces by CVD.



4/80 CD 19491

Figure 17. Load vs. Knoop hardness values of the surfaces on sputter-coated Be surface with  $0.3\mu$  B. (a) as sputter deposited, (b) after a heat treatment of  $1000^{\circ}\text{C}$  for 15 minutes.

## 2.6 Conclusions

The studies carried out during this reporting period lead us to the conclusion that the elements beryllium and boron react quite readily at temperatures 850°C or higher to form beryllium borides. However, both the beryllium surface and the environment in which the process is performed must be free of oxygen contamination. All the earlier failures to produce a bonded boride to beryllium substrate have been traced to the formation of an oxide layer at the interface. We have now improved our technique sufficiently to have been able to produce highly adherent thin layers of borides to the beryllium substrate by CVD. However, we have not completely eliminated the oxygen problem as indicated by the presence of oxygen seen in the Auger spectra depth profiles. It is quite possible that the presence of oxygen in the amount seen in these films may be responsible for the cracking and spalling of thicker films.

Thicker films are desirable for several reasons. First, they will make it possible to obtain definitive identification of phase or phases present, by x-ray diffraction technique. And if we find that we have produced the beryllium rich borides ( $\text{Be}_4\text{B}$  or  $\text{Be}_2\text{B}$ ) rather than the boron rich ones, the ability to produce adherent thicker films will be more conducive to the formation of boron rich borides, such as  $\text{BeB}_2$  or even  $\text{BeB}_6$ . It remains to be seen, however, whether it is necessary to form the boron rich films for gas bearing applications.

Even without the actual identification of phases in the CVD films of borides formed on the beryllium substrate we should be able to tell what we are forming on the basis of diffusion kinetics in the Be-B system. It has now become possible to begin such studies because of our success in two areas. First, we have been able to produce well-bonded diffusion couples by hot isostatic pressing technique. Secondly, using arc-plasma-spray on chilled copper substrate, we have produced solid pieces of  $\gamma$ -boron, which we consider very essential, but not available otherwise.

The presence of oxygen in our CVD films is of concern. We are continuing our studies to determine the source of oxygen, which will enable us to either eliminate or reduce its magnitude in our present system. If neither is possible using the present system we will have to give serious consideration to design and build a more sophisticated system to do so.

SECTION 3  
BERYLLIUM BORIDING BY ION IMPLANTATION

3.1 Background

Causing beryllium boride compounds to form in the surface of a beryllium component, in order to make that surface hard and wear resistant enough for use in a gas bearing, could conceivably be accomplished in a variety of ways. Several of these have been touched on in the preceding sections, with some mention of their characteristic advantages and disadvantages. One method which avoids some of the problems and uncertainties that could affect the more mature technologies is ion implantation processing.

The ion implantation process differs from those based on diffusion by virtue of its employment of kinetic, rather than thermal, energy to introduce and emplace the foreign species which is intended to modify the host material. A high kinetic energy is given to the species to be implanted, such as boron, by first ionizing the boron and then accelerating the ions through an electrical potential difference. They are then directed as a beam or current of ions onto a substrate material, such as beryllium, whose surface their high kinetic energy allows them to penetrate. The quantity of boron delivered is determined by the magnitude of the current (strictly speaking, the time-averaged ion current per unit area) and the length of time it is applied. The range of penetration of the ions depends on the accelerating potential. Consequently, for ion implantation processing the concentration of boron in the surface of the

beryllium is not limited by its solubility, and the penetration of boron into beryllium is not restricted either by the diffusivity of the boron or by the presence of any native oxide film on the beryllium. These characteristics are limiting factors in the more conventional boriding processes, however.

From the foregoing, it can be seen that a major feature of ion implantation is the control which it affords - control of quantity through control of both dose-rate (or ion current) and deposition time, and control of depth through adjustment of the acceleration voltage. In addition, practical ion implantation equipment and techniques provide for directing, rastering, or selective masking of the beam to allow precise placement of an implant in a given location. Also provided for would be the precise selection (i.e., high purity) of the element to be implanted, and a clean high-vacuum environment for protection of the surface being implanted.

Although the nominal solubility of boron in beryllium does not restrict the concentration that ion implantation can produce, the sputtering yield of beryllium (or any other substrate) under the bombardment of the incoming boron (or other) ions does set a limit. The basis for this can be grasped by considering that a material which sputters away rapidly during implantation would not be in place long enough to allow the build-up of a high concentration of the implanted species.

### 3.2 Progress Prior to This Reporting Period

Although the ion implantation process was not among those contemplated when this program was initiated, it began to receive some favorable consideration when the process which had been proposed originally began to show erratic results. These effects seemed possibly to be attributable to either a diffusion-inhibiting oxide film barrier on the beryllium, or to an unfavorable situation with respect to the diffusion rate of boron in beryllium relative to that of beryllium in boron. As noted above, the nature of ion implantation makes it virtually immune to either of these factors, so that it appeared to be an alternative worthy of investigation.

A preliminary trial,<sup>(6)</sup> carried out in a cooperative effort with the Materials Modification Branch of the Naval Research Laboratory, showed that a beryllium surface became measurably harder when implanted with boron to a concentration of 10 atomic per cent (10 a/o). Upon heat treatment at relatively low temperatures the implanted surface became harder still, an effect to be anticipated if beryllium boride compound formation were occurring, but not if the initial hardening were merely due to damage induced by ion bombardment during implantation. The actual observation was therefore very encouraging for the prospect of causing hard beryllium-boron compounds to form in the surface by ion implantation.

Equally encouraging was the preliminary indication that no detectable sputtering erosion had occurred at the beryllium surface. One implication of that finding is that, while the maximum attainable boron concentration is set by the sputtering yield of beryllium relative to that of boron under these conditions, the actual limit is quite high. Consequently here again prospects appear to be good for the conversion of a significant volume fraction of the surface region into one of the hard beryllium boride compounds. A second encouraging implication is that finished parts can be implanted without alteration of dimensions or surface finish.

### 3.3 Objectives

During the period of this report it was planned to implant additional specimens of I-400 beryllium to higher levels of boron concentration with a view to determining the upper limit attainable by this method, to characterize the surfaces so prepared as thoroughly as possible, and to observe their behavior under heat treatment. The information and data collected during such activity should be useful in any attempt to select optimum processing parameters for use in fabricating prototype gas bearings, if the results bore out the initial promising indications.

Appropriate characterization of the surfaces was seen as involving examination by optical and scanning electron microscopy to record the physical topography, and the use of electron diffraction in the transmission electron microscope to detect beryllium boride compound formation. Rutherford back-scattering\* was also expected to give information on compound formation; with the use of suitable calibration standards the same technique would permit refinement of estimates of implant concentration and of penetration depth and profile. Low-load (because of layer thinness) microhardness measurements on the processed specimens were seen as direct indicators of value as gas bearing materials, in addition to the usefulness of such measurements in physical characterization. As a final screening measure, short of actual prototype fabrication, friction and wear testing was planned.

#### 3.4 Progress in Fiscal Year 1979

Several factors combined to hold progress to a relatively modest level during this period.

It was mentioned above that the ion implantation work was for us a cooperative effort with the Naval Research Laboratory; it is anticipated that there will be long term and synergistic benefits for both organizations in that arrangement. However, it does mean that any equipment, personnel and scheduling problems affecting NRL also have a bearing on the progress of work at the Draper Laboratory.

The preliminary tests mentioned above were carried out in equipment designed for semiconductor electronics work, since until recently ion implantation has been almost exclusively a semiconductor processing

---

\* "Rutherford back-scattering", or RBS, is a non-destructive method of analyzing solid bodies. A mono-energetic beam of light ions (usually helium) in the megavolt energy range is directed at the test-specimen, and observation of the energy spectrum of the back scattered (helium) ions allows calculation (within limits) of the identity, quantity, and distribution of the atoms to be found within the test-specimen.

technique. However, semiconductor device fabrication requires doses much lighter than those contemplated here, so the use of such equipment for our work requires inordinately long times and is therefore an inefficient way to carry out metallurgical materials modification.

During the past year, NRL has been installing and debugging a new high current/high voltage ion implanter which is capable of practical, metallurgically significant, implantations. First deliveries of high-dose implantations produced with the new equipment are in the process of examination at this laboratory.

Specimens implanted to date have been of two different diameters, 3/8" and 3/4", with the former representing the specimen size treated in the low-current semiconductor-type processing equipment. Although such small areas are adequate for hardness testing, and preparation of samples for scanning electron microscopy and transmission electron microscopy, they are by no means adequate for friction and wear testing. The higher current (dose rate) capability of the new implanter permits treatment of the larger diameter specimens, which do permit friction and wear testing, in a reasonable length of time and with a high level of confidence that the entire surface has been exposed uniformly.

#### 3.4.1 Small Diameter (3/8") Specimen

Two of these were treated in the semiconductor-processing ion implanter, as follows: first one disc was given a series of doses uniformly covering one face, using four different energies to attain a concentration profile invariant with depth down to 0.8 - 1.0 microns total penetration. These doses were similar to those used for the earlier 10<sup>a</sup>/o implant except that the quantities were doubled to yield a layer containing 20 a/o boron. A second disc was then placed beside the first, with half of each masked off, and the implanting schedule was repeated. The result was a pair of specimens, each with two dosages - one containing 20 and 40<sup>a</sup>/o, the second having 0 and 20<sup>a</sup>/o - to allow comparisons of effects.

Microhardness measurements were taken at NRL in the "As Implanted" condition and repeated after the specimens were annealed at 650°C for 1 hour under a vacuum of  $10^{-6}$  Torr. The reported hardness values are listed in Table 2.

The data obtained for the 0/20 and 20/40 <sup>a</sup>/o implants discussed above are considered to be questionable, aside from their small diameters. It was noticed after the second implantation that the implanted portions of the two discs had taken on a brownish discoloration; upon annealing the discs, the brown areas became yellowish green with bands of other colors. NRL had assumed that the brown color was due to the decomposition of back-streamed vacuum-pump oil to yield a carbon deposit, but the behavior observed and color patterns seen suggest an oxide film. One possibility is that some of the tantalum platelet, used as a mask during the second implantation, was sputtered away by the boron ion bombardment during the implantation and deposited on the nearby beryllium surface. The subsequent oxidation of such a film would then produce the interference color bands, as were observed, characteristic of varying thickness of oxide. In any case, the data obtained for those specimens, especially in the colored areas, are not considered to be reliable since they do not represent beryllium which has been implanted only.

#### 3.4.2 Large Diameter (3/4 inch) Specimens

As was mentioned above, larger diameter discs than those used previously were needed if friction and wear measurements were to be carried out. A set of discs were cut from a 3/4 inch beryllium rod whose lot number was known and for which the chemical analysis and physical characterization were available. This was Brush Wellman I-400 Lot No. 4784 with 6.3% BeO, an average grain size of 8.0  $\mu\text{m}$ , and with other impurities and characteristics which are also typical of actual gyroscope material.

Table 2. Knoop hardness, 3/8 inch discs implanted in low current machine.

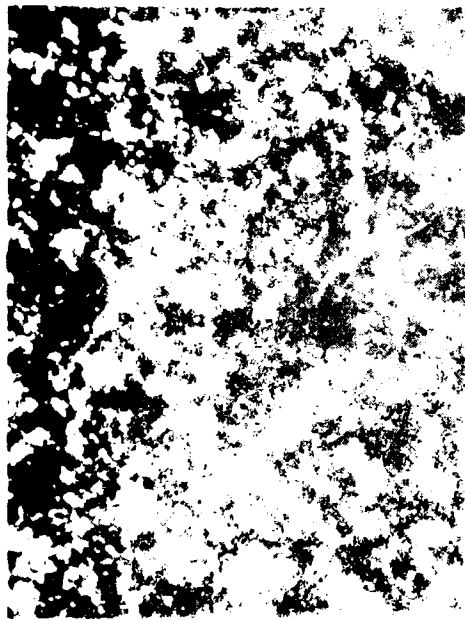
Load (grams)	Knoop Hardness									
	Unimplanted		20 <sup>a</sup> /o (a)		20 <sup>a</sup> /o (b)		40 <sup>a</sup> /o			
	650°C/1 hr		650°C/1 hr		650°C/1 hr		650°C/1 hr			
	Unannealed	Unannealed	Unannealed	Unannealed	Unannealed	Unannealed	Unannealed	Unannealed		
100	-	-	-	410	-	-	-	-	-	-
50	-	-	-	460	-	-	-	-	-	-
25	445	294	430	660	430	-	-	530	-	-
10	423	390	1010	900	-	-	-	1330	-	-
5	525	429	1090	-	-	-	-	2230	-	-
2	510	510	2850	-	-	-	-	4300	-	-
1	710	750	-	-	-	-	-	-	-	-

The first implantation performed on this set of substrates was nominally  $60 \text{ }^{\text{a}}/\text{o}$  with the same set of accelerating voltages as before, (i.e., selected to give a uniform concentration profile to a depth of about  $1 \text{ } \mu\text{m}$ . The specimen was subjected to Rutherford back-scattering (RBS) analysis and then delivered to CSDL for further testing. Also delivered was a small beryllium disc which had been implanted at the same time as the test specimen. The small disc had been half-masked to permit an assessment of thickness change during implantation (negative would show sputtering erosion; positive would show growth due to the volume change from the injection into the surface of the implanted boron).

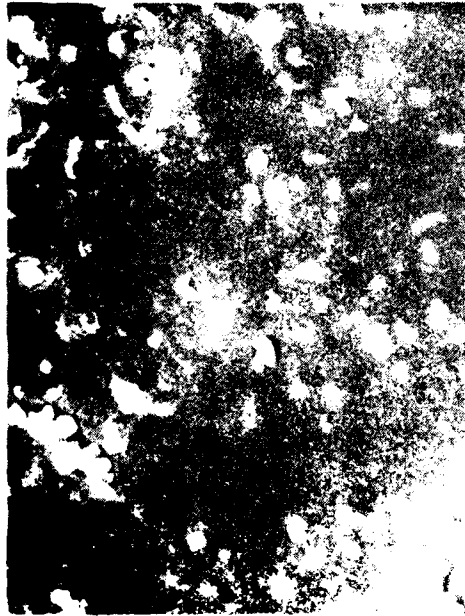
It is perhaps indicative of the evolutionary status of the technology that this " $60 \text{ }^{\text{a}}/\text{o}$ " specimen is also considered to be questionable. The RBS analysis appeared to show that the peak boron concentration was well below the nominal  $60 \text{ }^{\text{a}}/\text{o}$  while the surface (see Figure 18) is highly irregular and populated by various unexpected features. The small half-masked disc, on the other hand, appears to be much smoother and is relatively featureless.

Examination of the small disc both by optical interferometry and with a stylus-type profilometer indicated no observable height difference between the implanted and the unimplanted portions of the surface. It is surprising that no change occurred in either direction, but it may be that the growth due to the added material and the loss due to sputtering just compensate each other. A sputtering loss of approximately  $3000 \text{ \AA}$  during the  $60 \text{ }^{\text{a}}/\text{o}$  implantation would account for the observed behavior.

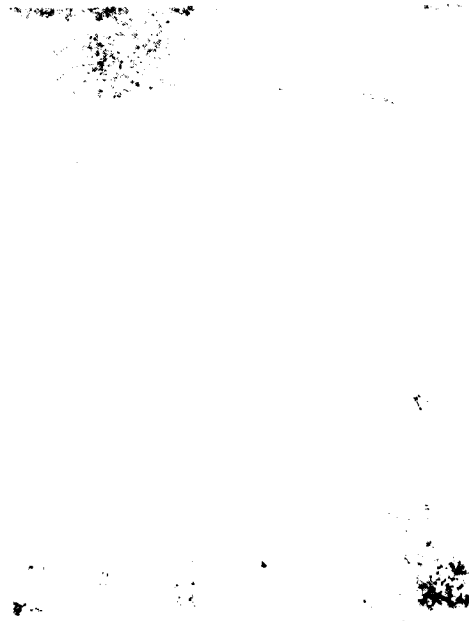
The most probable explanation of the strange performance of the larger disc is that it experienced a temperature excursion of unknown magnitude during the final, highest energy, dosage. With the fixturing available at the time the best that can be said is that the specimen temperature reached several hundred degrees. The small disc, being clamped under the half-mask, had a lower areal power dissipation and probably benefitted from better heat-sinking because of the clamping.



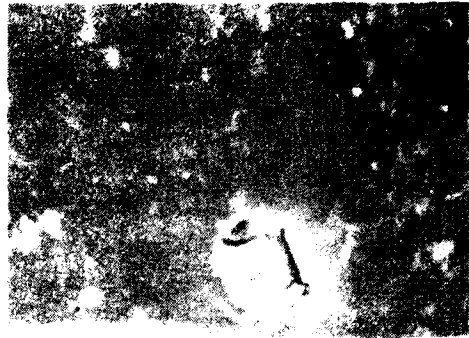
0.75 inch DISC



0.75 inch DISC



0.75 inch DISC



SMALL DISC



IMPLANTED



UNIMPLANTED

12/79 CD18716

Figure 18. 1-400 beryllium "60<sup>a</sup>/o" boron implantation.

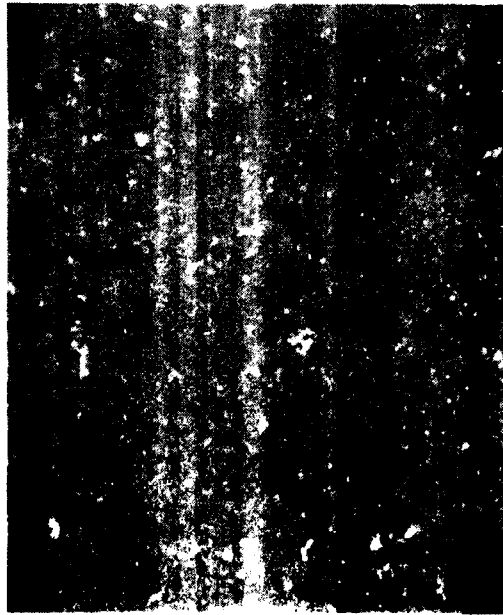
When the 40<sup>a</sup>/o specimen was prepared, procedures and fixturing had been improved to provide more positive heat dissipation, and more reliable temperature measurement with a thermocouple attached very near to the substrate. The specimen temperature probably did not exceed 190°C and possibly for that reason the surface is much smoother, as shown in Figure 19. While it is true that the dose was lower, 40<sup>a</sup>/o is still a very high dose and is at least the same order of magnitude as that delivered to the "60<sup>a</sup>/o" sample, so the surfaces should be similar.

Table 3 lists the values of Knoop hardness obtained at CSDL for the discs in the "As Implanted" condition. It may be seen that there is apparently little difference between these specimens, but in view of the uncertainty about the thermal history of the 60<sup>a</sup>/o implant it would be premature to draw conclusions at this time. A second specimen of that concentration, implanted with temperature control similar to the 40<sup>a</sup>/o sample, will give more reliable information.

### 3.5 Other Progress and Preparations

Much of the additional effort in this aspect of the gas bearing materials work has taken the form of refinements in equipment, technique and procedures. An example of this is the application of higher quality optics, including Nomarski phase contrast capability, to read and record the very small microhardness indentations needed to properly test very hard, thin films such as those resulting from ion implantation.

Secondly, a modification was designed and installed on the vacuum annealing furnace which permits rapid insertion, for post-implantation heat-treatment, of a specimen into the pre-heated furnace as well as rapid withdrawal at the end of the desired time interval. Both operations are performed without breaking the vacuum or gas-filled envelope. Previously, it was necessary to insert the specimen into the cold furnace, establish the vacuum or gas blanket, bring the furnace to temperature, and then cool it after a certain time interval before retrieving the sample. Precise specification of time/temperature conditions was therefore impossible.



0.75 inch DISC



0.75 inch DISC

Figure 19. I-400 beryllium 40 <sup>a</sup>/o boron implantation.

12/79 CD18717

Table 3. Knoop hardness, 3/4 inch discs implanted in high current machine, as implanted.

Load (grams)	Knoop Hardness Number	
	60 <sup>a</sup> / <sub>o</sub>	40 <sup>a</sup> / <sub>o</sub>
100	370	
50		413
25	603	
10	830	726
5	1033	1112

Finally, there is the development of a specimen flow sequence and handling procedure which will allow the most cost-effective use of the limited machine time available for this work at NRL, where access to the high current implanter is in great demand. It is as follows:

- (1) Beryllium disc preparation and polishing - CSDL
- (2) Boron ion implantation - NRL
- (3) RBS of "As Implanted" disc - NRL
- (4) Knoop hardness testing, "As Implanted" - CSDL
- (5) Electro-discharge machine (EDM) out, slice off and pre-thin an "As Implanted" surface sample for electron diffraction and microscopy - CSDL
- (6) Final thinning, and ED/TEM of "As Implanted" surface sample - NRL
- (7) Scanning electron microscopy (SEM) of "As Implanted" surface - CSDL
- (8) Friction and wear testing of "As Implanted" specimen (pin-on-disc; a single weartrack) - CSDL
- (9) Heat-treat specimen with precise time/temperature control - CSDL
- (10) CSDL repeats (4, 5, 7, 8 and 9) on the now "As Annealed" disc (8 is done at a different radius).
- (11) NRL repeats 3 and 6 on "As Annealed" samples

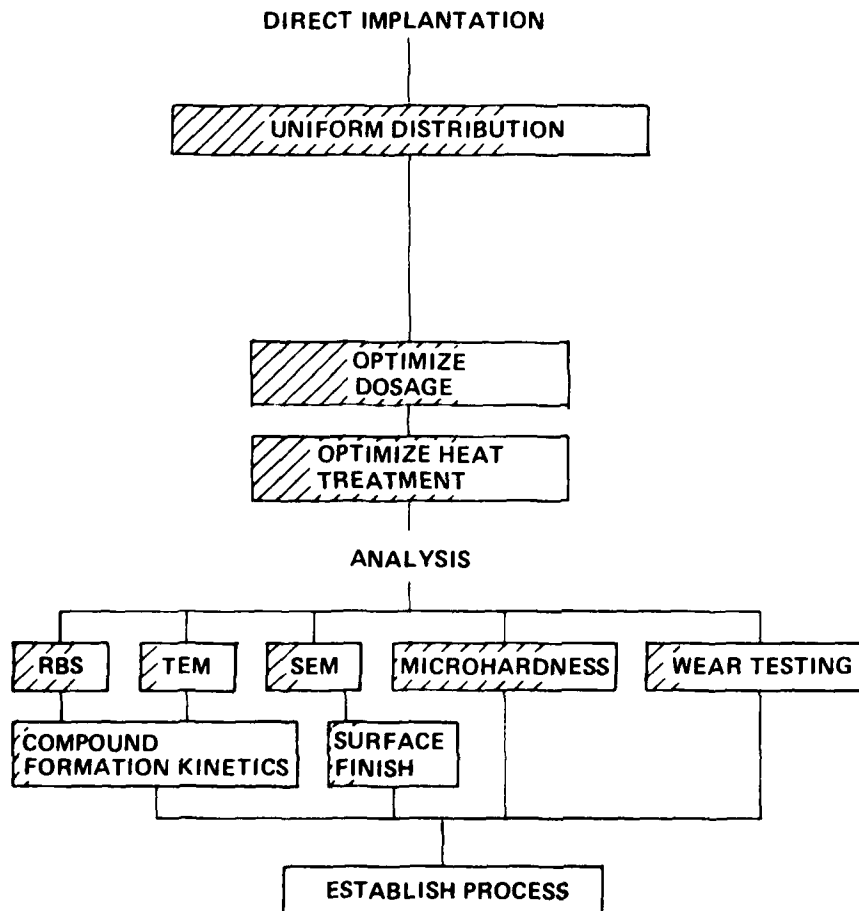
This scheme is expected to maximize the scientific data obtainable from a single exposure to the ion implantation equipment.

### 3.6 Direction of Future Work

Once the feasibility and fact of hard beryllium boride compound formation through ion implantation have been demonstrated, attention should be given to optimizing both the mechanical characteristics and the cost effectiveness. An approach which is seen as doing both would be the development of graded coatings; graded in boron concentration and graded in hardness, with the maximum of both at the gas-bearing surface.

Two methods of attaining graded coatings are believed to be practical. One of these would be all-implanted; it would feature a very heavy dose at low energy to establish a very hard wear surface, followed by lower doses at higher energies to provide a continuous decrease in brittleness and an increase in ductility with depth. This should enhance the ability of the structure to distribute surface stresses and impacts without material failure.

Much the same situation may be more easily attainable by the application of a film of boron to the beryllium surface, perhaps by sputter deposition, followed by a high energy boron implantation through the film. Several processes - recoil implantation, ion mixing, and deep subsurface implantation - could act simultaneously to produce the desired concentration and hardness gradient with no abrupt transitions or interfaces.



11/79 CD18464

Figure 20. Shaded area indicates degree of completion.

#### REFERENCES

1. Rutherford, J.L. and W.B. Swain, Alumina Bearing in Gas-Lubricated Gyros, AIAA/ASME 8th Structures, Structural Dynamics and Materials Conference, California, NASA Report No. NASA-CR-88597, 29-31 March 1967.
2. Advanced Inertial Technologies, Vol. III, Technical Report AFAL-TR-73-124, The Charles Stark Draper Laboratory, Inc., March 1974.
3. McEwen, J., and R. Schluntz, History and Experience into Chromium Oxide (LC-4) Plasma Coating of Bearings by Union Carbide, Report No. C-4699, The Charles Stark Draper Laboratory, Inc., July 1976.
4. Kumar, K., Analysis of W<sub>(x)</sub>C Sputter Deposits, Report No. C-4749, The Charles Stark Draper Laboratory, Inc., December 1976.
5. Keating, W.H., Compliance Coefficient Test Results for TGG No. 222X, Component Development Department Memorandum No. 30H-76-541, The Charles Stark Draper Laboratory, Inc., December 1976.
6. Palmieri, J., Gas Bearing Material Development by Surface Modification of Beryllium, Task 2 in Materials Research for Advanced Instrumentation, Technical Report R-1199, The Charles Stark Draper Laboratory, Inc., September 1978, (submitted to ONR under Contract N00014-77-C-0388).
7. Hoard, J.L., and A.E. Newkirk, "An Analysis of Polymorphism in Boron, etc.," J. Am. Chem. Soc., 82 (1960) 70.
8. Decker, B.F. and J.S. Kasper, "The Crystal Structure of a Simple Rhombohedral Form of Boron," ActaCryst, 12 (1959) 503.
9. Sands, D.E., and J.L. Hoard, "Rhombohedral Elemental Boron," J. Am. Chem. Soc. 79 (1957) 5582.

REFERENCES (Continued)

- (10) Laubengayer, D.T., D.T. Hurd, A.E. Newkirk, and J.L. Hoard, "Preparation and Properties of Pure Crystalline Boron," J. Am. Chem. Soc. 65, (1943) 1924.
- (11) Hoard, J.L., R.E. Hughes, and D.E. Sands, "The Structure of Tetragonal Boron," J. Am. Chem. Soc. 80 (1958) 4507.
- (12) Hoard, J.L., "Structure and Polymorphism in Elemental Boron," Advances in Chem, A.C.S., No. 32 (1961) 42.
- (13) Kumar, K. and D. Das, "Equilibrium and Metastable Samarium-Cobalt Deposits Produced by Arc-Plasma-Spraying," Thin Solid Films, Vol. 54, No. 3, p. 263 (1978).
- (14) Croft, W.J., N.C. Tombs, and J.F. Fitzgerald, "Preparation and Characterization of Boron Films from Diborane," Mat. Res. Bull, Vol. 5, p. 489 (1970).
- (15) Singhal, S.C., "An Erosion-Resistant Coating for Titanium and Its Alloys," Int. Conf. on Met. Coatings, San Francisco, California, 3-7 April 1978. To be published in "Thin Solid Films," 1978.

BASIC DISTRIBUTION LIST

Technical and Summary Reports April 1978

<u>Organization</u>	<u>Copies</u>	<u>Organization</u>	<u>Copies</u>
Defense Documentation Center Cameron Station Alexandria, VA 22314	12	Naval Air Propulsion Test Center Trenton, NJ 08628 ATTN: Library	1
Office of Naval Research Department of the Navy 800 N. Quincy Street Arlington, VA 22217		Naval Construction Battalion Civil Engineering Laboratory Port Hueneme, CA 93043 ATTN: Materials Division	1
ATTN: Code 471	1	Naval Electronics Laboratory	
Code 102	1	San Diego, CA 92152	
Code 470	1	ATTN: Electron Materials Science Division	1
Commanding Officer Office of Naval Research Branch Office Building 114, Section D 666 Summer Street Boston, MA 02210	1	Naval Missile Center Materials Consultant Code 3312-1 Point Mugu, CA 92041	1
Commanding Officer Office of Naval Research Branch Office 536 South Clark Street Chicago, IL 60605	1	Commanding Officer Naval Surface Weapons Center White Oak Laboratory Silver Spring, MD 20910 ATTN: Library	1
Office of Naval Research San Francisco Area Office 760 Market Street, Room 447 San Francisco, CA 94102	1	David W. Taylor Naval Ship Research and Development Center Materials Department Annapolis, MD 21402	1
Naval Research Laboratory Washington, DC 20375		Naval Undersea Center San Diego, CA 92132 ATTN: Library	1
ATTN: Codes 6000	1	Naval Underwater System Center	
6100	1	Newport, RI 02840	
6300	1	ATTN: Library	1
6400	1		
2627	1	Naval Weapons Center China Lake, CA 93555 ATTN: Library	1
Naval Air Development Center Code 302 Warminster, PA 18964 ATTN: Mr. F. S. Williams	1	Naval Postgraduate School Monterey, CA 93940 ATTN: Mechanical Engineering Department	1

BASIC DISTRIBUTION LIST (Continued)

<u>Organization</u>	<u>Copies</u>	<u>Organization</u>	<u>Copies</u>
Naval Air Systems Command Washington, DC 20360 ATTN: Codes 52031 52032	1	NASA Headquarters Washington, DC 20546 ATTN: Code RRM	1
Naval Sea System Command Washington, DC 20362 ATTN: Code 035	1	NASA (216) 433-400 Lewis Research Center 21000 Brookpark Road Cleveland, OH 44135 ATTN: Library	1
Naval Facilities Engineering Command Alexandria, VA 22331 ATTN: Code 03	1	National Bureau of Standards Washington, DC 20234 ATTN: Metallurgy Division	1
Scientific Advisor Commandant of the Marine Corps Washington, DC 20380 ATTN: Code AX	1	Inorganic Materials Division Director Applied Physics Laboratory University of Washington 1013 Northeast Fortieth Street Seattle, WA 98105	1
Naval Ship Engineering Center Department of the Navy Washington, DC 20360 ATTN: Code 6101	1	Defense Metals and Ceramics Information Center Battelle Memorial Institute 505 King Avenue Columbus, OH 43201	1
Army Research Office P.O. Box 12211 Triangle Park, NC 27709 ATTN: Metallurgy and Ceramics Program	1	Metals and Ceramics Division Oak Ridge National Laboratory P.O. Box X Oak Ridge, TN 37380	1
Army Materials and Mechanics Research Center Watertown, MA 02172 ATTN: Research Programs Office	1	Los Alamos Scientific Laboratory P.O. Box 1663 Los Alamos, NM 87544 ATTN: Report Librarian	1
Air Force Office of Scientific Research Bldg. 410 Bolling Air Force Base Washington, D.C. 20332 ATTN: Chemical Science Directorate Electronics and Solid State Sciences Directorate	1	Argonne National Laboratory Metallurgy Division P.O. Box 229 Lemont, IL 60439	1
Air Force Materials Laboratory Wright-Patterson AFB Dayton, OH 45433	1	Brookhaven National Laboratory Technical Information Division Upton, Long Island New York 11973 ATTN: Research Library	1

BASIC DISTRIBUTION LIST (Continued)

<u>Organization</u>	<u>Copies</u>	<u>Organization</u>	<u>Copies</u>
Library Building 50, Room 134 Lawrence Radiation Laboratory Berkeley, CA	1	Office of Naval Research Branch Office 1030 East Green Street Pasadena, CA 91106	1

SUPPLEMENTARY DISTRIBUTION LIST

<u>Organization</u>	<u>Copies</u>	<u>Organization</u>	<u>Copies</u>
Professor Peter Gielisse University of Rhode Island Division of Engineering Research Kingston, RI 02881	1	Professor David Turnbull Harvard University Division of Engineering and Applied Physics Cambridge, MA 02139	1
Mr. R. W. Rice Code 6360 Naval Research Laboratory 4555 Overlook Avenue, S.W. Washington, DC 20375	1	Dr. D. P. H. Hasselman Montana Energy and MHD Research and Development Institute P.O. Box 3809 Butte, MT 59701	1
Professor G. S. Ansell Rensselaer Polytechnic Institute Dept. of Metallurgical Engineering Troy, NY 12181	1	Dr. L. Hench University of Florida Ceramics Division Gainesville, FL 32601	
Professor J. B. Cohen Northwestern University Dept. of Material Sciences Evanston, IL 60201	1	Dr. J. Ritter University of Massachusetts Department of Mechanical Engineering Amherst, MA 01002	1
Professor M. Cohen Massachusetts Institute of Technology Department of Metallurgy Cambridge, MA 02139	1	Professor G. Sines University of California at Los Angeles Los Angeles, CA 90024	1
Professor J. W. Morris, Jr. University of California College of Engineering Berkeley, CA 94720	1	Director Materials Sciences Defense Advanced Research Projects Agency 1400 Wilson Boulevard Arlington, VA 22209	1
Professor O. D. Sherby Stanford University Materials Sciences Division Stanford, CA 94300		Professor H. Conrad University of Kentucky Materials Department Lexington, KY 40506	1
Dr. E. A. Starke, Jr. Georgia Institute of Technology School of Chemical Engineering Atlanta, GA 30332	1		

SUPPLEMENTARY DISTRIBUTION LIST (Continued)

<u>Organization</u>	<u>Copies</u>	<u>Organization</u>	<u>Copies</u>
Jack Bouchard Northrop/PPD 100 Morse Street Norwood, MA 02062	1	P. Jacobson Sperry Flight Systems P.O. Box 21111 Phoenix, AZ	1
Howard Schulien Department 6209 Bendix Corporation Guidance Systems Division Teterboro, NJ 07608	1	George R. Costello Senior Staff Engineer Control and Electromechanical Subdivision Guidance and Control Division The Aerospace Corporation P.O. Box 92957 El Segundo, CA 90009	1
Don Bates Honeywell, Inc. Aerospace Division 11350 U.S. Highway 19 St. Petersburg, FL 33733		John Hanks Dynamics Research Corp. 60 Concord Street Wilmington, MA 01887	1
R. Baldwin Honeywell, Inc. Avionics Division 2600 Ridgway Parkway Minneapolis, MN 55413	1	D. Riley Systems Group, Minuteman TRW Inc. P.O. Box 1310 San Bernardino, CA 92402	1
Bus Brady 62-11B/1 Lockheed Missile and Space Co., Inc. P.O. Box 504 Sunnyvale, CA 94088	1	Professor Robert Ogilvie Dept. of Materials Science and Engineering Massachusetts Institute of Technology Cambridge, MA 02139	1
Dan Fromm MS 1A1 Delco Electronics 7929 South Howell Avenue Milwaukee, WI 53201	1	Dr. Glen R. Buell (D. Starks) AFML/MBT Wright-Patterson Air Force Base Dayton, OH 45433	1
F. Mikoleit Autonetics Division Rockwell International 3370 Miraloma Avenue Anaheim, CA 92803	1	Major George Raroha AFAL/CC Wright-Patterson Air Force Base Dayton, OH 45433	

SUPPLEMENTARY DISTRIBUTION LIST (Continued)

<u>Organization</u>	<u>Copies</u>	<u>Organization</u>	<u>Copies</u>
Joe Jordan Litton Guidance and Control Systems 5500 Canoga Avenue Woodland Hills, CA 91364	1	Lt. Col. Gaylord Green Capt. Ken Wernle BMO/MNNG Norton Air Force Base San Bernardino, CA 92409	1
Bob Delaney Singer-Kearfott Division 150 Totowa Road Wayne, NJ 07470	1	Dave Gold (SP-230) Rick Wilson (SP-23411) Andy Weber (SP-23411) Strategic Systems Project Office Department of the Navy Washington, DC 20390	1
Elmer Whitcomb Sperry Gyroscope Division Great Neck, NY 11020	1	Lt. Col. Larry Fehrenbacker HQ/AFSC Andrews AFB, MD	1
C. Hoenig J. Holt R. Landingham Lawrence Livermore Laboratory University of California at Berkeley Livermore, CA 94550	1	N. Stuart (MMIRME) ALC/Ogden Ogden Air Logistics Command Hill AFB Ogden, UT 84404	1
Capt. S. Craig Aerospace Guidance Metrology Center Newark AF Station Newark, OH 43055	1	Professor R. M. Latanision Massachusetts Institute of Technology 77 Massachusetts Avenue Room E19-702 Cambridge, MA 02139	1
W. Lane Hamilton Standard Windsor Locks, CN	1	Dr. Jeff Perkins Naval Postgraduate School Monterey, CA 93940	1
Dr. A. G. Evans Dept. Material Sciences and Engineering University of California Berkeley, CA 94720	1	Dr. R. P. Wei Lehigh University Institute for Fracture and Solid Mechanics Bethlehem, PA 18015	1
Professor H. Herman State University of New York Material Sciences Division Stony Brook, NY 11794	1	Professor H.G. F. Wilsdorf University of Virginia Department of Materials Science Charlottesville, VA 22903	1
Professor J. P. Hirth Ohio State University Metallurgical Engineering Columbus, OH 43210	1		